

## Short Comments by Mark Vaughan

### Comments:

This paper compares the spatial and temporal distributions of the aerosol optical depths retrieved at 1064 nm by the CATS lidar aboard the International Space Station to the optical depths measured by AERONET (at 1020 nm) and the optical depths retrieved by MODIS and CALIOP (at 1064 nm).

This is the second version of this manuscript that I have read, but the first for which I've been asked to provide an invited (as opposed to contributed) review. My primary comment about this second version is that the authors' do not provide enough information for readers to confidently assess the quality of the CATS AOD estimates relative to those provided by the other sensors. In particular, relying on correlation coefficients alone to characterize the comparisons is insufficient. Consider the two series defined by  $y_2=2x$  and  $y_4 = 4x$ . While  $y_2$  and  $y_4$  are perfectly correlated – i.e., they have a correlation coefficient of 1 – in the mean,  $y_4$  is twice as large as  $y_2$ . So in addition to the correlation coefficients they already provide, the authors should also provide means and standard deviations for each of the datasets being compared. While Table 2 is a fine start, more is needed. In a similar vein, regarding figures 1 through 3, black-on-black overplotting of data points in high data density regions reduces the information content of the figures. So, in addition to the figures, the authors should also cite the descriptive statistics (e.g., min, max, median, mean, and standard deviation) for all datasets being compared. Furthermore, optical depths should be given (either in the text or, preferably, in the figure captions or legends) for all profiles plotted in figure 5 and figures 10–13. It is also my view that the authors have not responded sufficiently to several of the comments made by the original referees. Below I have listed the original referee comments together with the authors' responses and my criticisms of those responses. I hope the authors will revisit their original responses, and consider adding the additional requested by all referees. In addition to this review, I have attached an annotated version of the manuscript that contains a number of questions and suggestions. I hope to see responses to these issues reflected in the published version of this paper.

**Response:** *We really appreciate Mark Vaughan's valuable comments and made significant changes to this paper. We took the effort and have regenerated all the figures and tables using the newest version of CATS data (V3\_00). We find significant differences between raw V2-01 and V3 CATS aerosol products with outliers are significantly reduced in the raw V3 product. However, after the QA steps implemented in the study we found only marginal differences between V2-01 and V3 CATS aerosol products for this study. Most of the conclusions from this study remain largely unchanged after switching to the V3 CATS aerosol data. One plot (similar to Figure 1) is also included in the Appendix using V2-01 CATS aerosol data for a comparison purpose.*

*We have added density plots and included more descriptive statistical analyses (e.g. new tables 1 and 2) as suggested by Dr. Mark Vaughan. We have also included AODs in the figure captions for Figures 5, 10-11 as suggested. AODs for Figures 12 and 13 are included in the Table 3.*

*In addition, we have responded to detailed comments from the reviewer as below.*

## General Remarks

**Comments:** “Comments: Specific comments: Section 2, can you briefly describe the AOD measurement uncertainty of these instrument?”

Response: This is a great question. Most validation and uncertainties analysis efforts of satellite AOD retrievals are focus on visible channels. To our knowledge, uncertainties in AOD retrieval at 1064 nm, both from passive and active sensors, are less studied. Just as suggested from the comments from Mark Vaughan and Stuart Young (Short comment for this paper), this paper might be among the first to go deep into AOD retrievals at 1064 nm channel. We were not able to find papers to address uncertainties in AOD retrievals at 1064 nm, although there are papers that do show comparisons between CALIOP and AERONET AOD at 1064 nm (Omar et al., 2013). Omar, A. H., D. M. Winker, J. L. Tackett, D. M. Giles, J. Kar, Z. Liu, M. A. Vaughan, K. A. Powell, and C. R. Trepte (2013), CALIOP and AERONET aerosol optical depth comparisons: One size fits none, *J. Geophys. Res. Atmos.*, 118, 4748–4766, doi:10.1002/jgrd.50330. We have added the following discussion in the text: “Note that most evaluation efforts for passive- and active-based AOD retrievals are focused on the visible spectrum and the performance of AOD retrievals at the 1064 nm channel is less explored. “

I don’t think this response adequately addresses reviewer’s request. Estimating measurement uncertainties is not synonymous with validation; ideally, the former would always precede the latter. MODIS AOD uncertainties are explored in numerous papers (e.g., Tanré et al., 1997; Levy et al., 2003; Remer et al., 2005; and many others), and the same is true for AERONET aerosol retrievals (e.g., Holben et al., 1998; Dubovik et al., 2000; Sinyuk et al., 2012; and many others). Uncertainties in extinction and optical depth estimates retrieved using elastic backscatter lidars have a long history in the literature (e.g., Russell et al., 1997; Bissonnette, 1986; Jinhuan, 1988; Young, 1995; Del Guasta, 1998). In particular, the retrieval uncertainties for CALIOP are given in excruciating detail in Young et al., 2013. I’m not aware of any publication that specifically examines CATS extinction uncertainties. However, since CALIOP and CATS are both elastic backscatter lidars that use similar retrieval algorithms, I suspect that the material in Young et al., 2013 could easily be adapted to provide first-order estimates for the CATS uncertainties. I suspect the authors could make a useful response to this referee’s request in just 3 or 4 summary sentences.

## References

Bissonnette, L. R., 1986: Sensitivity analysis of lidar inversion algorithms, *Appl. Opt.*, 25, 2122–2125, doi:10.1364/AO.25.002122.

Del Guasta, M., 1998: Errors in the retrieval of thin-cloud optical parameters obtained with a two-boundary algorithm, *Appl. Opt.*, 37, 5522–5540, doi:10.1364/AO.37.005522.

Dubovik, O., A. Smirnov, B. N. Holben, M. D. King, Y. J. Kaufman, T. F. Eck, and I. Slutsker, 2000: Accuracy assessments of aerosol optical properties retrieved from Aerosol Robotic Network (AERONET) Sun and sky radiance measurements, *J. Geophys. Res.*, 105, 9791–9806, doi:10.1029/2000JD900040.

Holben, B. N., T. F. Eck, I. Slutsker, D. Tanre, J.P. Buis, A. Setzer, E. Vermote, J. A. Reagan, Y. J. Kaufman, T. Nakajima, F. Lavenu, I. Jankowiak and A. Smirnov, 1998: AERONET — A federated instrument network and data archive for aerosol characterization, *Rem. Sens. Env.*, 66, 1-16, doi:10.1016/S0034-4257(98)00031-5.

Jinhuan, Q., 1988: Sensitivity of lidar equation solution to boundary values and determination of the values, *Adv. Atmos. Sci.*, 5, 229–241, doi:10.1007/BF02656784.

Levy, R. C., L. A. Remer, D. Tanré, Y. J. Kaufman, C. Ichoku, B. N. Holben, J. M. Livingston, P. B. Russell and H. Maring, 2003: Evaluation of the Moderate-Resolution Imaging Spectroradiometer (MODIS) retrievals of dust aerosol over the ocean during PRIDE, *J. Geophys. Res.*, 108, 8594, doi:10.1029/2002JD002460.

Remer, L. A., Y. J. Kaufman, D. Tanre, S. Mattoo, D. A. Chu, Martins, J. V., Li, R. R., Ichoku, C., Levy, R. C., R. G. Kleidman, T. F. Eck, E. Vermote, and B. N. Holben , 2005: The MODIS aerosol algorithm, products, and validation, *J. Atmos. Sci.*, 62, 947–973, doi:10.1175/JAS3385.1.

Russell, P. B., T. J. Swissler, and M. P. McCormick, 1979: Methodology for error analysis and simulation of lidar aerosol measurements, *Appl. Opt.*, 22, 3783–3797, doi:10.1364/AO.18.003783.

Sinyuk, A., B. N. Holben, A. Smirnov, T. F. Eck, I. Slutsker, J. S. Schafer, D. M. Giles and M. Sorokin, 2012: Assessment of error in aerosol optical depth measured by AERONET due to aerosol forward scattering, *Geophys. Res. Lett.*, 39, L23806, doi:10.1029/2012GL053894.

Tanré, D., Y. J. Kaufman, M. Herman and S. Mattoo, 1997: Remote sensing of aerosol properties over oceans using the MODIS/EOS spectral radiances, *J. Geophys. Res.*, 102 (D14), 16971–16988, doi:10.1029/96JD03437.

Young, S. A., 1995: Analysis of lidar backscatter profiles in optically thin clouds, *Appl. Opt.*, 34, 7019-7031, doi:10.1364/AO.34.007019.

Young, S. A., M. A. Vaughan, R. E. Kuehn, and D. M. Winker, 2013: The Retrieval of Profiles of Particulate Extinction from Cloud-Aerosol Lidar Infrared Pathfinder Satellite Observations (CALIPSO) Data: Uncertainty and Error Sensitivity Analyses, *J. Atmos. Oceanic Technol.*, 30, 395-428, doi:10.1175/JTECH-D-12-00046.1.

**Response:** *We have included discussions of uncertainties in various places relating to different data products.*

*“AERONET does not have specific guidance on error in the 1020 nm channel, as it is known to have some thermal sensitivities. However, they do report significantly more confidence in version 3 of the data, which has temperature correction (Giles et al., 2018). Error models are ongoing, and for this study we assume double the RMSE, or +/-0.03.”*

*“While the uncertainties in MODIS infrared (e.g. 1240 nm) retrievals are less explored, the reported over ocean MODIS DT AOD retrievals are  $+(0.04 + 0.1*AOD, -(0.02 + 0.1*AOD))$  for the green channel (levy et al., 2013). “*

*“The uncertainties in retrieved aerosol extinction, as suggested by Young et al., (2013), is around  $0.05–0.5 \text{ km}^{-1}$  for the 532 nm channel. Validated against AERONET data, Omar et al., (2013) suggested that 74% and 81% of the CALIOP AOD retrievals are fall within the expected*

*uncertainties ( $0.05+0.4*AOD$ ) as suggested by Winker et al., (2009) for the 1064nm channel, for all sky and clear sky conditions respectively.”*

*“Although the uncertainties in CATS aerosol retrievals have not yet been documented for the CATS V3-00 extinction and AOD products, much like CALIOP, uncertainties in the calibration and assumed lidar ratios are the primary contributors to the extinction and AOD uncertainties. The uncertainties in the CATS 1064 nm attenuated total backscatter (ATB) is on the order of 7-10% for nighttime and is around 20% for daytime (Pauly et al., 2019), while the uncertainties in the assumed 1064 nm lidar ratios for CATS are 30%. Thus, the CATS 1064 nm extinction (40-70%) and AOD (30-50%) uncertainties are very similar to the corresponding CALIOP’s 1064 nm uncertainties.”*

**Comment:** Comments: P8, L163, can you describe what constant value of that Angstrom exponent is used here without letting readers to look for that in Shi et al. paper?

Response: We apologize for the confusion. The Angstrom exponent values are computed using instantaneous retrievals. We have revised the text to avoid confusion.

*“Here we assume the angstrom exponent value, computed using instantaneous AOD retrievals at the 860 and 1240 nm, remains the same for the 860 to 1064 nm wavelength range, similar to what has been suggested by Shi et al., (2011; 2013).”*

Please provide a representative range (e.g., mean and standard deviation or some other common statistical description) of the Ångström exponents actually used.

**Response:**

*Mean and standard deviation were added to the text as suggested.*

*“Mean and standard deviation of Ångström exponents using this method were 0.69 and 0.55, respectively.”*

**Comment:** Comments: Can you provide an explanation on why the AOD measured by CATS less than all other instruments suggested by Figure 1, 2, and 3?

Response: We assume that the reviewer is referring to the slope of the regressions in Figures 1-3. Slopes in linear regressions can often be biased by outliers. In Figure 6, which are spatial plots of AODs from CALIOP and CATS, differences are less noticeable for the DJFMAM season. For the JJASON season, CATS AODs are lower at certain regions (Middle East, India, and North Africa) and higher over other regions (South Africa). The cause of those discrepancies, however, is unclear to us. To really explore the issue, it deserves a paper of its own. Thus, we leave this topic to a future paper

I’m quite perplexed by this response. First, if the slopes are not trustworthy indicators of the correlation between the two data sets, why report them at all? Or, if the authors are concerned that “slopes in linear regressions can often be biased by outliers”, why didn’t they remove any obvious outliers before plotting their data and computing and reporting the values of the slopes? Second, and perhaps more important, there’s at least one plausible and obvious answer to the reviewer’s question. According to Rebecca Pauly’s CATS calibration paper, the CATS attenuated backscatter coefficients are biased low by ~19% relative both to ground-based Polly measurements and to CALIOP measurements. This low bias in the attenuated backscatter coefficients will invariably lead to low biases in the retrieved optical depths (see the section on

calibration and renormalization errors in Young et al., 2013).

(Full disclosure: I am a back-of-the-pack coauthor on Rebecca Pauly's CATS calibration paper.) In my opinion, this comment should be fully addressed in this paper, and not postponed to some future paper. There are several reasons why “the AOD measured by CATS [might be] less than all other instruments”, and the authors should make a good faith attempt to enumerate and discuss at least the most obvious of those reasons.

**Response:** *Note that based on the slopes of the regression lines shown in Figures 1-3, AODs retrieved by CATS are less than AERONET, CALIOP and DT Aqua MODIS AOD retrievals. As shown in Table 1, however, for the one-to-one collocated datasets, mean CATS AODs (1064 nm) are ~10% higher than AERONET AODs (1020 nm). The CATS AODs are ~3% higher than CALIOP AOD (1064 nm) and are ~5-10% higher than DT MODIS AODs. One possible explanation for this discrepancy is because mean AODs are dominated by low AOD cases and the slopes of the regression relationships are strongly affected by a few high AOD cases. Thus, it is likely that CATS AODs are overestimated at the low AOD ranges and are underestimated at the high AOD ranges. We have included the following discussions in the text.*

*“Note that based on the slopes of the regression lines shown in Figures 1-3, AODs retrieved by CATS are less than AERONET, CALIOP and DT Aqua MODIS AOD retrievals. As shown in Table 1, however, for the one-to-one collocated datasets, mean CATS AODs (1064 nm) are ~10% higher than AERONET AODs (1020 nm). The CATS AODs are ~3% higher than CALIOP AOD (1064 nm) and are ~5-10% higher than DT MODIS AODs. One possible explanation for this discrepancy is because mean AODs are dominated by low AOD cases and the slopes of the regression relationships are strongly affected by a few high AOD cases. Thus, it is likely that CATS AODs are overestimated at the low AOD ranges and are underestimated at the high AOD ranges.”*

**Comment:** Comments: (5) The aerosol extinction at 1064 nm may not be as sensitive to the fine mode aerosols (such as smoke and urban pollutant aerosols) compared to the coarse mode aerosols (such as dust). The authors probably should add a few sentences to address this  
Response: Great point. We have added the following discussions to address this issue. “Still, readers shall be aware that AOD retrievals at the 1064 nm are less sensitive to fine mode aerosols such as smoke and pollutant aerosols, compared to coarse mode aerosols such as dust aerosols. Thus, an investigation of diurnal variations of aerosol properties at the visible channel may be also needed for a future study.”

A reference for the first statement would make a very nice addition to the paper.

**Response:** *We have added a reference (e.g. Dubovik et al., 2000)*

**Comment:** Short Comments by Mark Vaughan and Stuart Young (table 2)

I strongly suggest adding standard deviations to this table; the observed variability of the AODs provides a critically important point of comparison between the two sets of retrievals. I also

suggest adding a table comparing CATS means and standard deviations to the AERONET and MODIS means and standard deviations.

**Response:** *We have added standard deviations to Table 2 (now new table 3). We have also added new tables 1 and 2 as suggested.*

**Comment:** While I did not expect the authors to do a complete reanalysis of their data, I had hoped to see a bit more in-depth discussion of the uncertainties inherent in this kind of simple temporal and spatial matching technique and some discussion, perhaps, on how these might be mitigated. For example, the authors use version 3 level 2 AERONET data in their study, whereas the Omar et al., 2013 analysis used version 2 level 2 AERONET data. Are there improvements between versions 2 and 3 that might reduce the differences in the cloudiness inferred by AERONET versus the cloudiness observed by coincident space-based lidar measurements?

**Response:** *We have included a detailed study of the comparisons between CATS AODs and AODs from other instruments (CALIOP, AERONET and MODIS). This include varying of both spatial and temporal collocation windows (new Table 2). Only marginal differences, however, are found from this exercise. We have included in the following discussions.*

*“Also note that as suggested by Omar et al., (2013), the choices of spatial and temporal collocation windows have an effect on collocation results. Thus, we repeated the exercises in Figures 1-3 by doubling the spatial and temporal collocation windows as well as reducing the collocation windows by half. The descriptive statistics of this sensitivity study is included in Table 2. While the number of collocated data pairs are drastically affected by the spatial and temporal collocation window sizes, less significant changes, however, are found in descriptive statistics such as mean, median, and standard deviations of AODs, as well as slopes and correlation values. The slope of DT Aqua MODIS and CATS AODs, however, seems sensitive to changes in collocation methods. Changes in slope of 0.61 to 0.78 are found for the change of temporal collocation window from 15 minutes to 60 minutes with a fixed spatial collocation window of 0.4 °Latitude/Longitude. “*

*One of the design purposes of the V3 AERONET data is to reduce thin cirrus cloud contamination. We have also included the following discussions:*

*“Note that Version 3 AERONET data are designed to reduce thin cirrus cloud contamination as well as rescue heavy aerosol scenes that were misclassified as clouds in previous versions (e.g. Gail et al., 2019).“*

**Comment:** Comment: Furthermore, given the lower CATS AODs shown in Figure 2, it's surprising to see that the CATS extinctions coefficients shown in Figure 5 are typically larger than CALIOP at all altitudes, and that the closest agreement is over land (where CATS slightly underestimates CALIOP at lower altitudes). Again, some discussion of the possible causes of this paradox would be welcome.

Response: First, there is a call from the community to avoid using slopes from the regression analysis as they are prone to noisy data, and we are kind of agree with them. Statistically, we

expect a high percentage of small AODs versus large AODs. Still, slopes are dominated by high AOD cases, while the averaged profiles may be more dominated by low AOD cases. This could explain the difference.

This response helped motivate my “primary comment” in the opening paragraphs of this review. Given that slopes (and correlation coefficients) are imperfect metrics, additional statistical parameters should be given to more fully characterize the comparisons between the different datasets.

**Response:** *We have included detailed descriptive statistics for Figures 1-3 as suggested. Interestingly, the mean CATS AOD is ~3% higher than the mean CALIOP AOD for the collocated CALIOP and CATS data (see prior response to this). Thus, it is not surprising that “CATS extinction coefficients shown in Figure 4 are typically larger than CALIOP at all altitudes.”*

**Comment:** Comment: The CATS extinction profiles shown in Figures 5 and 10 peak at altitudes some hundreds of meters higher than do CALIOP’s, except over land. While CALIOP’s profiles show almost no roll off until about the last range bin above the surface, the CATS profiles start dropping off below about 500 m, or at approximately 8 to 9 range bins above the surface. What is happening here? Is CATS altitude registration and/or surface detection the culprit? Or is the cloud filter too aggressive in the boundary layer (i.e., are strongly scattering aerosols being misclassified as clouds)? Irrespective of the underlying cause(s), is this behavior a major source of AOD differences between CATS and CALIOP?

Response: The 2 biggest issues in the CATS V2-01 data were the daytime calibration and the daytime cloud-aerosol discrimination. A CATS paper in preparation (Yorks et al., 2019) has included details about the cloud-aerosol discrimination issues, while Rebecca Pauly’s 1064 nm calibration paper has a lot of details about the new daytime calibration. We have checked this issue by reprocessing the analysis using 3 months of V3 data and we found an improvement in agreement for AOD, but with some differences still evident in the vertical profiles.

While this is a helpful explanation, I do not see where it appears in the revised paper. Given that the CATS V3 data is now publicly available, I think it’s essential to include some information that relates these findings to the currently available CATS data.

**Response:** *We took the time and actually reworked on the paper using V3 CATS data. However, the above mentioned discrepancy still exist. We have suspected the following reasons and included them in the paper:*

*“Due to the precessing orbit of the ISS, the CATS sampling is irregular and very different compared to the sun-synchronous orbits of the A-Train sensors. These orbital differences between CATS and CALIOP make comparing the data from these two sensors challenging since they are fundamentally observing different locations of the Earth at different times. Thus, we shouldn’t expect the extinction profiles and AOD from these two sensors to completely agree. Additionally, there are other algorithm and instrument differences that can lead to differences in extinction coefficients and AOD. Over land where dust is the dominant aerosol type, differences in lidar ratios between the two retrieval algorithms (CATS uses 40 sr while CALIOP uses 44 sr), can cause CATS extinction coefficients that are up to 10% lower than CALIOP, potentially explaining the higher CALIOP extinction values in Figure 5e. Over ocean, especially during daytime, differences*

in CATS and CALIOP lidar ratios for marine and smoke aerosols can introduce a difference between CATS and CALIOP extinction coefficients (Figure 5d). These difference in over ocean data (Figure 5d) could also attributed to differences in CATS and CALIOP 1064 nm backscatter calibration. For example, Pauly et al. (2019) reports that CATS attenuated total backscatter is about 19.7% lower than PollyXT measurements in the free troposphere and 19% lower than CALIOP of opaque cirrus clouds due to calibration uncertainties for both sensors.

**Comment:** Comment: The seasonal maps (Figure 6) show that the CALIOP AODs exceed those of CATS over the Arabian Peninsula, and to a smaller degree over the African region bordering the Gulf of Guinea. Can this also be explained by differences in lidar ratio selection, or are there other factors at work?

*Response:* We suspect the difference in retrieval method as mentioned above may contribute. Also, CALIOP provides early morning and afternoon overpasses while CATS can observe at near all solar hours, the differences may also be associated with these sampling differences. Again, I do not see where this helpful explanation appears in the revised manuscript.

**Response:** It is included:

*“Those discrepancies may result from biases in each product, but it is also possibly due to the differences in satellite overpass times, as CALIOP provides early morning and afternoon over passes, and Aqua MODIS has an over pass time after local noon, while CATS is able to report atmospheric aerosol distributions at multiple times during a day. ”*

**Comment:** Comment: page 8, line 163: logarithmic interpolation, correct? Also, please state the actual value of the Ångström exponent given by Shi et al.

*Response:* Yes. The Angstrom exponent value is computed for each AOD retrieval. We have revised the discussion to avoid confusion. “Here we assume the angstrom exponent value, computed using instantaneous AOD retrievals at the 860 and 1240 nm, remains the same for the 860 to 1064 nm wavelength range, similar to what has been suggested by Shi et al., (2011; 2013).”

To repeat an earlier comment, please provide a representative range (e.g., mean and standard deviation or some other common statistical description) of the Ångström exponents actually used. Don't leave your readers guessing and/or wondering about what values you used in deriving your 1064 nm AOD estimates.

**Response:** Done (see prior response to this).

**Comment:** Comment: page 8, line 170: while “AERONET data are considered as the ground truth for evaluating CATS retrievals”, it should be noted that there are very few AERONET sites in remote oceans. Do MODIS retrievals substitute as the gold standard in these places?

*Response:* Even though a better performance can be expected from MODIS aerosol retrievals over ocean versus over land, we still think that only AERONET data should be used for ground truth, as instantaneous retrievals from passive sensors suffer from various issues such as cloud contamination.

This is not a very useful response, mostly because AERONET, like MODIS, is a passive sensor and thus also suffers from “various issues such as cloud contamination” (e.g., Chew et al., 2011 and Huang et al., 2011). Taking the authors’ response at face value, the number of opportunities for ground truth over ocean must be vanishingly small relative to the number of over-ocean measurements being evaluated.

#### References

Chew et al., 2011: Tropical cirrus cloud contamination in sun photometer data, *Atmos. Environ.*, 45, 6724-6731, <https://doi.org/10.1016/j.atmosenv.2011.08.017>

Huang et al., 2011: Susceptibility of aerosol optical thickness retrievals to thin cirrus contamination during the BASE-ASIA campaign *J. Geophys. Res.*, 116, D08214, doi:10.1029/2010JD014910.

**Response:** *The version 3 AERONET data were used in this study. One of the design purposes of the Version 3 AERONET data is to reduce the uncertainties in thin cirrus cloud contamination (Giles et al., 2019). Also, although there are fewer AERONET stations available over global oceans, the Maritime Aerosol Network expended the existing ground-based AERONET observations through ship-borne aerosol measurement.*

*Still, we understood that there are uncertainties in AERONET AOD retrievals and we have documented that in the paper and added the following discussions.*

*“Note that Version 3 AERONET data are designed to reduce thin cirrus cloud contamination as well as rescue heavy aerosol scenes that were misclassified as clouds in previous versions (e.g. Gail et al., 2019).”*

*Giles, D. M., Sinyuk, A., Sorokin, M. G., Schafer, J. S., Smirnov, A., Slutsker, I., Eck, T. F., Holben, B. N., Lewis, J. R., Campbell, J. R., Welton, E. J., Korkin, S. V., and Lyapustin, A. I.: Advancements in the Aerosol Robotic Network (AERONET) Version 3 database – automated near-real-time quality control algorithm with improved cloud screening for Sun photometer aerosol optical depth (AOD) measurements, *Atmos. Meas. Tech.*, 12, 169-209, <https://doi.org/10.5194/amt-12-169-2019>, 2019.*

**Comment:** Comment: page 9, line 186-187: some discussion on the rationale for the choices of  $\pm 0.4^\circ$  and  $\pm 30$  minutes would be helpful in evaluating the strength of the comparisons.

Reponses: We picked this threshold following a few previous papers (e.g. Toth et al., 2018). We have added discussions in the text to further clear this issue:

*“Note that as suggested by Omar et al., 2013, the choices of spatial and temporal collocation windows have an effect on collocation results. However, we consider this as a topic beyond the scope of this study”*

See my previous remarks on this response.

**Response:** *We have done a detailed sensitivity analysis by varying the spatial and temporal collocation windows for Figures 1-3. The details are included in Table 2.*

-----  
**Comments from the marked paper**  
-----

**Comment:** Line 64, “not sure what this means; is there a word (or multiple words) missing here?”

**Response:** *We have changed "phenomena" to "characteristics" to avoid confusion*

**Comment:** Line 71, “since CATS is no longer operational, replace "flying" with "that flew”

**Response:** *Done*

**Comment:** Lines 110-112, “what does this mean; i.e., what does QC\_Flag = 0 tell me about the extinction and/or optical depth retrieval?”, “please don't force readers to dig up the CATS ATBD in order to understand the meanings of these quality flags. instead, add brief descriptions in the text.”, “please explain the significance of feature type scores between -2 and -10?”

**Response:** *The descriptions of the quality flags have been added to the text. The feature type score is similar to the CALIOP CAD score, and is a probability density function-based numerical confidence level. The magnitude indicates the confidence (-10 is complete confidence, 0 is as likely to be cloud as aerosol).*

**Comment:** Lines 147-148, “why does CALIOP use 0, 1, 2, 16, and/or 18 when CATS only uses 0? what's the difference in these QC flags?”, “to repeat a previous comment, please don't force readers to dig up the CALIOP ATBDs in order to understand the meanings of these quality flags. instead, add brief descriptions in the text.”

**Response:** *The descriptions of the quality flags have been added to the text. This is a great point. We had used those CALIOP flags as they were used in previous work by Campbell et al., 2012, but in order to be consistent between the two sensors for this study, we have modified this to include only CALIOP Extinction\_QC\_Flag\_1064 is equal to 0 (initial lidar ratio unchanged). This did not have a large impact on the results.*

**Comment:** Lines 163-165, “specify the range of Ångström exponents (e.g., mean and standard deviation, or median and 10% and 90% deciles) you derived from these many instantaneous retrievals. also, replace "angstrom" with "Ångström”

**Response:** *Done (see prior response on this).*

**Comment:** Line 182, “use "passive and active sensor" rather than "passive and active based”?”

**Response:** *Done*

**Comment:** Line 185, “undefined acronym”

**Response:** *Defined DT as "Dark Target"*

**Comment:** Line 186, “CATS”

**Response:** *Done.*

**Comment:** Lines 186-187, “what does "not derived in this study" mean?”

**Response:** *We deleted the sentence to avoid confusion.*

**Comment:** Line 193, “doesn't that cover the entire CATS mission lifetime? since a study covering the whole mission lifetime is about as comprehensive as could be, it might be worth pointing this out.”

**Response:** *As suggested. We have added "the entire mission" in the text.*

**Comment:** Line 208, “you could help other folks that might want to use CATS data by saying which of the QA steps were most effective in removing the large AODs”

**Response:** *In CATS Version 2, by far the most effective step was limiting the 1064 nm Extinction Coefficient to less than  $1.25 \text{ km}^{-1}$ . However, with the improvements in the CATS Version 3 dataset, this is no longer as clear cut. Still, for a 1% reduction in the number of passes, correlation coefficient between CATS and AERONET is improve from 0.51 to 0.65, standard deviation is reduced from 0.15-0.21 to 0.10-0.12, and several outliers of high CATS AOD/low AERONET AOT are removed. Requiring the Extinction QC flag to be equal to 0 and the Extinction Uncertainty to be less than  $10 \text{ km}^{-1}$  had the largest impacts on reducing the difference in mean and medians of the AERONET and CATS AOD, with a loss of only 4 passes out of 2270 (less than 0.2% reduction in passes) for each threshold.*

*We added in the text, “We also found that requiring the Extinction QC flag to be equal to 0 and the Extinction Uncertainty to be less than  $10 \text{ km}^{-1}$  had the largest impacts on reducing the difference in mean and medians of the AERONET and CATS AOD. “*

**Comment:** Lines 214-215, “hence the utility of describing which of the QA steps were most effective in winnowing out unsuitable values”

**Response:** *See prior comment on this.*

**Comment:** Line 220 “if you interpolate/rescale the MODIS data, why don't you also interpolate/rescale the AERONET data?”

**Response:** *AERONET data include observations at 1020 nm, which is close to 1064nm CATS wavelength, and we expect comparable values for AOD for the two wavelengths. The adjacent MODIS retrievals are at 870 and 1240 nm, thus an interpolation is needed as we expect large changes in AOD from 1020 nm to either 870 nm or 1240 nm.*

**Comment:** Line 226, “please clarify; are MODS 1064 nm AOD estimates obtained via linear interpolation between 870 nm and 1240 nm, or by logarithmic interpolation? make this explicit in the text.”

**Response:** *We have added "logarithmic" and "again, assuming the aerosol Ångström Exponent value remains unchanged from 0.87 to 1.064  $\mu\text{m}$  as well as from 1.064  $\mu\text{m}$  to 1.24  $\mu\text{m}$  spectral channels" in the text*

**Comment:** Line 239, “more importantly, CALIOP and CATS are both elastic backscatter lidars (though there are significant differences in instrument design)”

**Response:** *We have added the change as well as included the sentence "Note that despite difference in instrumental designs, CALIOP and CATS are both elastic backscatter lidars."*

**Comment:** Line 246, “disagree; providing some assurance and/or assessment of an apples-to-apple comparison is an essential part of the evidence that should be presented”

**Response:** *We have conducted a detailed sensitivity study relating to collocation window sizes (Table 2). Related discussions are also included as mentioned in a previous response.*

**Comment:** Line 256, “CALIOP daytime 1064 nm data is slightly noisier than CALIOP nighttime 1064 nm data. CATS daytime 1064 nm data is substantially noisier than CATS nighttime 1064 nm data.”

**Response:** We removed “expected to be” as suggested. We didn’t include the suggested comment as we are unaware of a paper that we can cite for this comment.

**Comment:** Line 258, “a useful adjunct to the AOD study would be a companion study that compared mean vertical extents of the aerosols detected by the two instruments. how much of the AOD differences can be attributed to simple layer detection differences? (this can be answered in part by computing the mean extinction coefficients rather than the mean AODs.)”

**Response:** Nice suggestion. Still, the difference in AOD could be attributed to many factors, including cloud screening, uncertainties in various observed and modeled parameters used in the retrieval process

including lidar ratio, as well as other factors. It is a study of its own and thus we didn't explore the issue further.

**Comment:** Line 262, "clouds are not "accurately detected by the CATS data products". instead, the CATS data products report the detection results achieved by the CATS retrieval algorithms and software."

**Response:** *We have rewritten the sentence as "the feature type score can be used for clouds screening throughout the diurnal envelope of solar angles" to avoid confusion.*

**Comment:** Line 263, "reconsider this statement; CATS day vs. night differences in SNR pretty much guarantee that there will be some day vs. night detection biases."

**Response:** *We have rewritten the sentence as "To further evaluate impact of the solar contamination introduced bias in the diurnal analysis in aerosol detection or products, CATS AODs are evaluated as a function of local time."*

**Comment:** Line 266, "ugly sentence structure; see the comment from the original Vaughan & Young review referencing the Alan Robock article in EOS ("Parentheses are (are not) for references and clarification (saving space)")"

**Response:** *We have revised the sentence as suggested.*

**Comment:** Lines 281-282, "are the differences statistically significance? please comment."

**Response:** *Comparing the mean AOD at local midnight to the mean AOD at local noon by performing a student's t test, the difference is not significant at the 95% confidence level, with a p-value of 0.16.*

*We have added the following discussions.*

*"Still, comparing the mean AOD at local midnight to the mean AOD at local noon by performing a student's t test, the difference is not significant at the 95% confidence level, with a p-value of 0.16. "*

**Comment:** Line 304, "disagree; the comparison in 5c does not look substantially better than those shown in 5a, 5b, or 5d. reporting the optical depths calculated from each of these profiles might help clarify."

**Response:** *We have rewritten the sentence to "As shown in Figure 5e, a reasonable agreement is found between CATS V3-00 aerosol extinction with CALIOP for over land"*

**Comment:** Line 307, "why is this relegated to an appendix?"

the x-axis limits on this plot should be tightened up considerably.  $\pm 0.05$  would be much, much better and much, much more revealing of the differences between the two data sets."

**Response:** *This figure has been added to the main text (Figure 5f), and the axes limited to  $\pm 0.05$  as suggested.*

**Comment:** Line 308, “undefined acronym”

**Response:** *Since we use V3 CATS data now, the discussion was deleted.*

**Comment:** Line 315, “undefined acronym”

**Response:** *Since we use V3 CATS data, the discussion was removed*

**Comment:** Line 316, “need to modify this sentence; CATS V3-00 data was publicly released 31 October 2018. see [https://eosweb.larc.nasa.gov/project/cats/l2\\_table](https://eosweb.larc.nasa.gov/project/cats/l2_table)”

**Response:** *Since we use V3 CATS data, the discussion was removed*

**Comment:** Line 331, “I don't see this paper in the list of references”

**Response:** *Added.*

*Yorks, J. E., P.A. Selmer, E.P. Nowottnick, S.D. Rodier, M.A. Vaughan, N. Dacic, M.J. McGill, and S.P. Palm, CATS Level 2 Vertical Feature Mask Algorithms and Data Products: An Overview and Initial Assessment, Atmos. Meas. Tech. Discuss., in preparation, 2019.*

**Comment:** Line 337, “no. according to the abstract in the Pauly paper, CATS mean attenuated backscatter is  $\sim 19.7\%$  lower than PollyXT measurements in the free troposphere and  $\sim 19\%$  lower than CALIOP measurements of opaque cirrus clouds. that the differences are essentially the same when comparing to measurements made by two different instruments using two different targets suggests that the CATS calibration is responsible for the discrepancies seen in this example.”

**Response:** *Done. We have revised the sentence to “Pauly et al. (2019) reports that CATS attenuated total backscatter is about 19.7% lower than PollyXT measurements in the free troposphere and 19% lower than CALIOP of opaque cirrus clouds due to calibration uncertainties for both sensors.”*

**Comment:** Lines 342-343, “what explains the very different shapes of the CATS and CALIOP profiles in the lowest 250 m? the authors should discuss this.”

**Response:** *Differences in the lowest 250 m between CATS and CALIOP extinction profiles are due to how the instrument algorithms detect the surface and near-surface aerosols. Both the CATS and CALIOP feature detection algorithms create a gap between the surface and near-surface aerosol base altitude, despite the possible presence of aerosols in this altitude region.*

*CALIOP has an aerosol base extension algorithm that is designed to (1) detect scenarios when aerosols are present in the bins just above the surface and (2) extend the near-surface aerosol layer base down to the surface (Tackett et al., 2018). However, CATS does not use such an algorithm so false regions of “clear-air” exist between the surface and near-surface aerosol layers.*

*Tackett, J. L., Winker, D. M., Getzewich, B. J., Vaughan, M. A., Young, S. A., and Kar, J.: CALIPSO lidar level 3 aerosol profile product: version 3 algorithm design, Atmos. Meas. Tech., 11, 4129-4152, <https://doi.org/10.5194/amt-11-4129-2018>, 2018.*

*We have added the discussion in the text.*

*“Also, differences in the lowest 250 m between CATS and CALIOP extinction profiles are observable, which are due to how the instrument algorithms detect the surface and near-surface aerosols. Both the CATS and CALIOP feature detection algorithms create a gap between the surface and near-surface aerosol base altitude, despite the possible presence of aerosols in this altitude region. CALIOP has an aerosol base extension algorithm that is designed to (1) detect scenarios when aerosols are present in the bins just above the surface and (2) extend the near-surface aerosol layer base down to the surface (Tackett et al., 2018). However, CATS does not use such an algorithm so false regions of “clear-air” exist between the surface and near-surface aerosol layers.”*

**Comment:** Line 348, “did the authors require that there be a minimum number of extinction samples in each range bin? if so, what was that number?”

**Response:** *We did not require a minimum number for these range bins.*

**Comment:** Line 362, “are both daytime and nighttime retrievals used to construct these figures? please include this information.”

**Response:** *The figures include both daytime and nighttime retrievals for Figure 6-9. This has been added to the section describing the creation of these Figures.*

*“Both daytime and nighttime retrievals are included in this figure, as well as Figures 7-9.”*

**Comment:** Line 381, “in addition to mean values, also report the standard deviations”

**Response:** *Since we use V3 CATS data now, the discussion was deleted.*

**Comment:** Line 382, “do these maps of MODIS AODs include only those values that are coincident with the CALIOP footprints? i.e., was the MODIS averaging done in such a way that we should expect a near one-to-one match with the CALIPSO AODs?”

**Response:** *All MODIS data that passed QA steps were used in creating Figures 6a and 6b. Thus, we do not expect a one-to-one match with CALIOP AODs.*

*We added "using all available MODIS DT retrievals that passed QA steps as described in Section 2.3"*

**Comment:** Line 384, "patterns"

**Response:** *Changed to "patterns" suggested.*

**Comment:** Line 400, change to "nearly"

**Response:** *Done*

**Comment:** Lines 408-409, "I don't understand how this conclusion can be drawn from the evidence presented. CATS doesn't retrieve estimates of background aerosol AOD, does it?"

**Response:** *we deleted this sentence*

*"as global means are dominated by background aerosols that have weak diurnal variations in measured absolute AOD values"*

**Comment:** Line 447 "would be helpful if the text used the same time format that's used in the figure legends (e.g., 6:00 PM vs. 1800)"

**Response:** *We have updated the figure legend to use the same time format as the text to be consistent as suggested.*

**Comment:** Line 447 "is this behavior consistent with AOD patterns seen in AERONET measurements?"

**Response:** *Due to spatial and temporal sampling differences, we didn't pursue this question. E.g., AERONET AODs are column integrated values. Thus it is hard to inter-compare AERONET AODs with CATS extinctions below 1 km.*

**Comment:** Line 457-458, "something seems to be missing in this sentence; should it say "so that a near one-to-one transformation..."???"

**Response:** *We revised the sentence to:*

*"Note a near 1 to 1 transformation can be achieved between UTC and local solar time."*

**Comment:** Line 460, "should this be "seasonal"?"

**Response:** *Corrected*

**Comment:** Line 465, “unsightly sentence construction again; heed the Robock comment

**Response:** *We revised the sentence to :*

*“Regional-based analyses are also conducted for 4 selected regions for the DJFMAM season and 5 selected regions for the JJASON season“*

**Comment:** Line 484,” suggest revising this; "local morning" at 00:00 AM would more commonly be known as "midnight".”

**Response:** *Changed to "midnight”*

**Comment:** Line 714,-716 table 2, “add standard deviations in addition to means”

**Response:** *Done for the new Table 3.*

**Comment:** Figure 1, “black-on-black overplotting of points in high data density regions reduces the information content of the figures. so in addition to the figures, cite the descriptive statistics (e.g., min, max, median, mean, and standard deviation) for all datasets being compared”

**Response:** *Done. Also included descriptive statistics in Tables 1 & 2.*

**Comment:** Figure 2, “lack-on-black overplotting of points in high data density regions reduces the information content of the figures. so in addition to the figures, cite the descriptive statistics (e.g., min, max, median, mean, and standard deviation) for all datasets being compared”

**Response:** *Done. Also included descriptive statistics in Tables 1 & 2.*

**Comment:** Figure 3, “black-on-black overplotting of points in high data density regions reduces the information content of the figures. so in addition to the figures, cite the descriptive statistics (e.g., min, max, median, mean, and standard deviation) for all datasets being compared”

**Response:** *Done. Also included descriptive statistics in Tables 1 & 2.*

**Comment:** Figure 5, “the integrals of each profile would be very helpful in assessing the differences, and should be reported either in the text or in the figure caption”

**Response:**

*We have added the mean AOD values, which are directly derived from and proportional to the integrals of the profiles, to the caption for Figure 5.*

**Comment:** Figure A1, “why is this relegated to an appendix?”

the x-axis limits on this plot should be tightened up considerably.  $\pm 0.05$  would be much, much better and much, much more revealing of the differences between the two data sets.”

**Response:** *Done (see previous response to this).*

1  
2  
3  
4  
5  
6  
7  
8  
9  
10  
11  
12  
13  
14  
15  
16  
17  
18  
19  
20  
21  
22  
23  
24  
25

**Investigation of CATS aerosol products and application toward global diurnal variation of aerosols**

Logan Lee<sup>1</sup>, Jianglong Zhang<sup>1</sup>, Jeffrey S. Reid<sup>2</sup>, and John E. Yorks<sup>3</sup>

<sup>1</sup>Department of Atmospheric Sciences, University of North Dakota, Grand Forks, ND

<sup>2</sup>Marine Meteorology Division, Naval Research Laboratory, Monterey, CA

<sup>3</sup>NASA Goddard Space Flight Center, Greenbelt, MD

Submitted to

ACP

Dec. 2018

Corresponding Author: [jzhang@atmos.und.edu](mailto:jzhang@atmos.und.edu); [logan.p.lee@und.edu](mailto:logan.p.lee@und.edu)

26

### Abstract

27 We present a comparison of 1064 nm aerosol optical depth (AOD) and aerosol extinction profiles  
28 from the Cloud-Aerosol Transport System (CATS) Level 2 aerosol product with collocated  
29 Aerosol Robotic Network (AERONET) AOD, Aqua and Terra Moderate Imaging  
30 Spectroradiometer (MODIS) Dark Target AOD and Cloud-Aerosol Lidar with Orthogonal  
31 Polarization (CALIOP) AOD and extinction data for the period of Feb. 2015-Oct. 2017. Upon  
32 quality assurance checks of CATS data, reasonable agreement is found between aerosol data from  
33 CATS and other sensors. Using quality assured CATS aerosol data, for the first time, variations  
34 in AODs and aerosol extinction profiles are evaluated at 00, 06, 12, and 18 UTC (and/or 0:00 am,  
35 6:00 am, 12:00 pm and 6:00 pm local solar times) on both regional and global scales. This study  
36 suggests that marginal variations are found in AOD from a global mean perspective, with the  
37 minimum aerosol extinction values found at 6:00 pm (local time) near the surface layer for global  
38 oceans, for both the June-November and December-May seasons. Over land, below 500m, the  
39 daily minimum and maximum aerosol extinction values are found at 12:00pm and 00:00/06:00 am  
40 (local time), respectively. Strong diurnal variations are also found over North Africa and India for  
41 the December-May season, and over North Africa, South Africa, Middle East, and India for the  
42 June-November season.

43

44

45 **1.0 Introduction**

46 Aerosol measurement through the sun-synchronous orbits of Terra and Aqua by nature  
47 encourages a larger scale, daily average point of view. Yet, we know that pollution (e.g., Zhao et  
48 al., 2009; Tiwari et al., 2013; Kaku et al., 2018), fires and smoke properties (e.g., Reid et al., 1999;  
49 Giglio et al., 2003; Hyer et al., 2013), and dust (e.g., Mbourou, et al., 1997; Fielder et al., 2013;  
50 Heinold et al., 2013) can exhibit strong diurnal behavior. Sun-synchronous passive satellite  
51 aerosol observations from the solar spectrum only provide a small sampling of the full diurnal  
52 cycle. Geostationary sensors such as the Advanced Himawari Imager (AHI) on Himawari 8  
53 (Yoshida et al., 2018) and Advanced baseline Imager on GOES-16/17 (Aerosol Product  
54 Application Team of the AWG Aerosols/Air Quality/Atmospheric Chemistry Team, 2012)  
55 satellites, while an improvement over their predecessors, must overcome the broader range of  
56 scattering and zenith angles (Wang et al., 2003; Christopher and Zhang, 2002) with no nighttime  
57 retrievals. Aerosol RObotic NETwork (AERONET; Holben et al., 1998) based sun photometer  
58 studies improve sampling, but until very recently with the development of a prototype lunar  
59 photometry mode, are also limited to daylight hours. The critical early morning and evening are  
60 largely missed in solar observation based approaches.

61 Observations of the diurnal variations of aerosol properties are needed for improving  
62 chemical transport modeling, geochemical cycles and ultimately climate. The measurement of  
63 diurnal variations of aerosol properties resolved in the vertical is especially crucial of aerosol  
64 characteristics for visibility and particulate matter forecasts. Indeed, the periods around sunrise  
65 and sunset show significant near surface variability that is difficult to detect with passive sensors.  
66 While lidar data from Cloud-Aerosol Lidar with Orthogonal Polarization (CALIOP) provide early  
67 afternoon and morning observations, two temporal points and a 16-day repeat cycle are insufficient

68 to evaluate the critical morning and evening hours where many key aerosol lifecycle processes  
69 take place.

70           Some of the limiting factors in previous studies can be addressed by the Cloud-Aerosol  
71 Transport System (CATS) lidar that flew aboard the International Space Station (ISS) since 2015  
72 (McGill et al. 2015). The ISS's precessing orbit with a 51.6° inclination allows for 24 hour  
73 sampling of the tropics to mid-latitudes, with the ability to observe aerosol and cloud vertical  
74 distributions at both day and night time with high temporal resolution. For a given location within  
75 ±51.6° (Latitude), after aggregating roughly 60 days of data, near full diurnal cycle of aerosol and  
76 cloud properties can be obtained from CATS observations (Yorks et al. 2016). This provides a  
77 new opportunity for studying diurnal variations (day and night) in aerosol vertical distributions  
78 from space observations.

79           Use of CATS has its own challenges. Most importantly, CATS retrievals must cope with  
80 variable solar noise around the solar terminator where we expect some of the strongest diurnal  
81 variability to exist. Further, CATS lost its 532 nm channel early in its deployment, leaving only a  
82 1064 nm channel functioning. The availability of only one wavelength limited the CATS cloud-  
83 aerosol discrimination algorithm, which can cause a loss of accuracy compared to CALIPSO  
84 which has 2 wavelengths. This deficiency is in part overcome by using the Feature Type Score  
85 (CATS Algorithm Theoretical Basis Document). Using two years of observations from CATS, in  
86 this paper, we focus on understanding of the following questions: How well do CATS derived  
87 aerosol optical depth (AOD) and aerosol vertical distributions compare with aerosol properties  
88 derived from other ground-based and satellite observations such as AERONET, MODIS and  
89 CALIOP? Do differences exhibit a diurnal cycle? What are the diurnal variations of aerosol optical

90 depth on a global domain? What are the diurnal variations of aerosol vertical distribution on both  
91 regional and global scales?

92

## 93 **2.0 Datasets**

94 Four datasets, including ground-based AERONET data, as well as satellite retrieved  
95 aerosol properties from MODIS and CALIOP, are used for inter-comparing with AOD and aerosol  
96 vertical distributions from CATS. Upon thorough evaluation and quality assurance procedures,  
97 CATS data are further used for studying diurnal variations of AOD and aerosol vertical  
98 distributions for the period of Feb. 2015 – Oct. 2017.

99

## 100 **2.1 CATS**

101 CATS Level 2 (L2) Version [3-00](#) 5 km Aerosol Profile products ([L2O D-M7.2-V3-](#)  
102 [00 05kmPro](#), [L2O N-M7.2-V3-00 05kmPro](#)) were used in this study for the entire period of  
103 CATS operation on the ISS (~Feb. 2015–Oct. 2017). CATS L2 profile data [is](#) provided at 5 km  
104 along-track horizontal resolution and 533 vertical levels at 60 m vertical resolution and a  
105 wavelength of 1064 nm. CATS also provides data at 532 nm, but due to a laser-stabilization issue,  
106 532 nm data is not recommended for use (Yorks et al. 2016). Thus, only 1064 nm products were  
107 used in this study. [Although the uncertainties in CATS aerosol retrievals have not yet been](#)  
108 [documented for the CATS V3-00 extinction and AOD products, much like CALIOP, uncertainties](#)  
109 [in the calibration and assumed lidar ratios are the primary contributors to the extinction and AOD](#)  
110 [uncertainties. The uncertainties in the CATS 1064 nm attenuated total backscatter \(ATB\) is on the](#)  
111 [order of 7-10% for nighttime and is around 20% for daytime \(Pauly et al., 2019\), while the](#)  
112 [uncertainties in the assumed 1064 nm lidar ratios for CATS are 30%. Thus, the CATS 1064 nm](#)

113 extinction (40-70%) and AOD (30-50%) uncertainties are very similar to the corresponding  
114 CALIOP's 1064 nm uncertainties.

115 CATS data are quality-assured following a manner similar to Campbell et al. (2012), which  
116 was applied to CALIOP. QA thresholds (including extinction QC flag, Feature Type Score, and  
117 uncertainty in extinction coefficient) are listed below:

118 (a) Extinction\_QC\_Flag\_1064\_Fore\_FOV is equal to 0 (non-opaque layer; lidar ratio  
119 unchanged)

120 (b) Feature\_Type\_Fore\_FOV = 3 (contains aerosols only)

121 (c)  $-10 \leq \text{Feature\_Type\_Score\_FOV} \leq -2$  (Feature Type Score < 0 is aerosol, with -10  
122 being complete confidence, and 0 being as likely to be cloud as aerosol)

123 (d) Extinction\_Coefficient\_Uncertainty\_1064\_Fore\_FOV  $\leq 10 \text{ km}^{-1}$

124 Extinction was also constrained using a threshold as provided in the CATS data catalog  
125 (Extinction\_Coefficient\_1064\_Fore\_FOV  $\leq 1.25 \text{ km}^{-1}$ ), similar to several previous studies  
126 (Redemann et al., 2012; Toth et al., 2016). Only profiles with extinction coefficient values less  
127 than  $1.25 \text{ km}^{-1}$  are included in this study. Small negative extinction coefficient values, however,  
128 are included in aerosol profile related analysis, to reduce potential high biases in computed mean  
129 profiles. Note that a similar approach has also be conducted in deriving passive-based AOD  
130 climatology (e.g. Remer et al., 2005). For this study, both the  
131 Aerosol\_Optical\_Depth\_1064\_Fore\_FOV and Extinction\_Coefficient\_1064\_Fore\_FOV datasets  
132 were used to provide AOD and 1064 nm extinction profiles (hereafter the term “extinction” will  
133 refer to 1064 nm unless explicitly stated otherwise), respectively.

## 135 **2.2 CALIOP**

136 NASA's CALIOP is an elastic backscatter lidar that operates at both 532 nm and 1064 nm  
137 wavelengths (Winker et al., 2009). Being a part of the A-Train constellation (Stephens et al.,  
138 2002), CALIOP provides both day- and night-time observations of Earth's atmospheric system, at  
139 a sun-synchronous orbit, with a laser spot size of around 70 m and a temporal resolution of ~16  
140 days (Winker et al., 2009). For this study, CALIOP Level 2.0 Version 4.1 5 km Aerosol Profile  
141 products (L2\_05kmAProf) are used for inter-comparing to CATS retrieved AODs and aerosol  
142 vertical distributions.

143 L2\_05kmAProf data are available at 5 km horizontal resolution along-track and include  
144 aerosol retrievals at both 532 nm and 1064 nm wavelengths. The vertical resolution is 60 m near-  
145 surface, degrading to 180 m above 20.2 km in MSL altitude. As only 1064 nm CATS data are  
146 used in this study as mentioned above, likewise only those CALIOP parameters relating to 1064  
147 nm are used in this study (Vaughan et al., 2018; Omar et al., 2013). Note that as suggested by  
148 Rajapakshe et al. (2017), lower signal-to-noise ratio (SNR) and higher minimum detectable  
149 backscatter are found for the CALIOP 1064 nm data in-comparing with the CALIOP 532 nm data.  
150 Also, the CALIOP aerosol layers are detected at 532 nm and the 1064 nm extinction is only  
151 computed for the bins within these layers. This may introduce a bias for aerosol above cloud  
152 studies. The uncertainties in retrieved aerosol extinction, as suggested by Young et al., (2013), is  
153 around 0.05–0.5 km<sup>-1</sup> for the 532 nm channel. Validated against AERONET data, Omar et al.,  
154 (2013) suggested that 74% and 81% of the CALIOP AOD retrievals are fall within the expected  
155 uncertainties (0.05+0.4\*AOD) as suggested by Winker et al., (2009) for the 1064nm channel, for  
156 all sky and clear sky conditions respectively.

157 In this study, Extinction\_Coefficient\_1064 and  
158 Column\_Optical\_Depth\_Tropospheric\_Aerosols\_1064 are used for CALIOP extinction and AOD

159 retrievals, respectively (Vaughan et al., 2019; Omar et al., 2013). As with the CATS data, CALIOP  
160 data are quality-assured following the quality assurance steps as mentioned in a few previous  
161 studies (e.g. Campbell et al., 2012; Toth et al., 2016; 2018). These QA thresholds are listed below:

162 (a) Extinction\_QC\_Flag\_1064 is equal to 0 ([unconstrained retrieval: initial lidar ratio](#)  
163 [unchanged](#))

164 (b) Atmospheric\_Volume\_Description = 3 or 4 ([contains aerosols only](#))

165 (c)  $-100 \leq \text{CAD\_Score} \leq -20$  ([CAD < 0 is aerosol, with -100 being complete confidence,](#)  
166 [and 0 being as likely to be cloud as aerosol](#))

167 (d) Extinction\_Coefficient\_Uncertainty\_1064  $\leq 10 \text{ km}^{-1}$

168 Furthermore, as in Campbell et al. (2012), only those profiles with AOD > 0 were retained  
169 in order to avoid profiles composed of only retrieval fill values. Extinction was also constrained  
170 to the nominal range provided in the CALIOP data catalog (Extinction\_1064  $\leq 1.25 \text{ km}^{-1}$ ),  
171 similar to our QA procedure for CATS as described above.

172

### 173 **2.3 MODIS Collection 6.1 Dark Target product**

174 Moderate Resolution Imaging Spectroradiometer (MODIS) Aqua and Terra Collection 6.1  
175 Dark Target over-ocean AOD data (Levy et al., 2013) were used for comparison to CATS AOD.  
176 The data field of “Effective\_Optical\_Depth\_Best\_Ocean” were used and only those data flagged  
177 as “good” or “very good” by the Quality\_Assurance\_Ocean runtime QA flags are selected for this  
178 study, similar to Toth et al. (2018). Because MODIS does not provide AOD in the 1064 nm  
179 wavelength, AOD retrievals from 860 and 1240 nm spectral channels are used to logarithmically  
180 interpolate AODs at 1064 nm. Here we assume the [Ångström Exponent](#) value, computed using  
181 instantaneous AOD retrievals at the 860 and 1240 nm, remains the same for the 860 to 1064 nm

182 wavelength range, similar to what has been suggested by Shi et al., (2011; 2013). Mean and  
183 standard deviation of Ångström exponents using this method were 0.69 and 0.55, respectively.  
184 Only totally cloud free (or cloud fraction equal to zero) retrievals, as indicated by the  
185 Cloud\_Fraction\_Land\_Ocean parameter are used. While the uncertainties in MODIS infrared  
186 (e.g. 1240 nm) retrievals are less explored, the reported over ocean MODIS DT AOD retrievals  
187 are  $+(0.04 + 0.1 \cdot \text{AOD})$ ,  $-(0.02 + 0.1 \cdot \text{AOD})$  for the green channel (levy et al., 2013).  
188

Moved (insertion) [2]

## 189 2.4 AERONET

190 By measuring direct and diffuse solar energy, AERONET observations are used for  
191 retrieving AOD and other ancillary aerosol properties such as size distributions (Holben et al.,  
192 1998). AERONET data are considered as the ground truth for evaluating CATS retrievals in this  
193 study. Only cloud screened and quality assured version 3 level 2 AERONET data at the 1020 nm  
194 spectrum are selected and are used for inter-comparing with CATS AOD retrievals at the 1064 nm  
195 wavelength. AERONET does not have specific guidance on error in the 1020 nm channel, as it  
196 is known to have some thermal sensitivities. However, they do report significantly more  
197 confidence in version 3 of the data, which has temperature correction (Giles et al., 2019). Error  
198 models are ongoing, and for this study we assume double the RMSE, or +/-0.03. Note that Version  
199 3 AERONET data are designed to reduce thin cirrus cloud contamination as well as rescue heavy  
200 aerosol scenes that were misclassified as clouds in previous versions (e.g. Gail et al., 2019).  
201

## 202 3.0 Results & Discussion

### 203 3.1 Inter-comparison of CATS data with AERONET, MODIS and CALIOP data

204 Note that most evaluation efforts for passive and active sensor AOD retrievals are focused  
205 on the visible spectrum and the performance of AOD retrievals at the 1064 nm channel is less  
206 explored. Thus, in this sub-section, the performance of over land and over ocean CATS AOD  
207 retrievals are compared against AERONET and C6.1 over ocean MODIS Dark Target (DT)  
208 aerosol products. In AOD related studies, CATS and CALIOP reported AOD values are used.  
209 However, only AOD values with corresponding aerosol vertical extinction that meet the QA  
210 criteria as mentioned in Sections 2.1 and 2.2 were used. CATS derived aerosol extinction vertical  
211 distributions are also cross-compared against collocated CALIOP aerosol extinction vertical  
212 distributions.

213

### 214 3.1.1 CATS-AERONET

215 As the initial check, CATS data from the entire mission (Feb. 2015-Oct. 2017) were  
216 spatially (within 0.4 degree Latitude and Longitude) and temporally ( $\pm 30$ minutes) collocated  
217 against ground-based AERONET data. Note that one AERONET measurement may be associated  
218 with several CATS retrievals in both space and time, and vice versa. Thus, both CATS and  
219 AERONET data were further averaged spatially and temporally, which results in only one pair of  
220 collocated and averaged CATS and AERONET data for a given collocated incident. Also, only  
221 data pairs with AOD larger than 0 from both instruments are used for the analysis. This step is  
222 necessary to exclude CATS profiles with all retrieval fill values as discussed in Section 2 (Toth et  
223 al., 2018). Such profiles containing all retrieval fill values were found to make up approximately  
224 5.3% of all CATS profiles in the dataset. Note that the CATS-AERONET comparisons are for  
225 daytime only, and higher uncertainties are expected for CATS daytime than nighttime AODs.

226 As shown in Figure 1a, without quality-assurance procedures, high spikes in CATS AOD  
227 of above 1 (1064 nm) can be found for collocated AERONET data with AOD less than 0.4 (1020  
228 nm). Still, those high spikes in CATS AOD are much reduced compared to the V2-01 CATS  
229 aerosol products (e.g. a similar plot as Figure 1 is included in the Appendix A with the use of V2-  
230 01 CATS aerosol data). Upon completion of the QA steps as outlined in Section 2.1, a reasonable  
231 agreement is found between quality-assured CATS (1064 nm) vs. AERONET (1020 nm) AODs  
232 with a correlation of 0.65 (Figure 1b). Comparing Figure 1a with 1b, with the loss of only ~1-2%  
233 of collocated pairs due to the QA procedures, we have observed an overall improvement in  
234 correlation between CATS and AERONET AOD from 0.51 to 0.64, thus, only QAed CATS data  
235 are used hereafter. We also found that requiring the Extinction QC flag to be equal to 0 and the  
236 Extinction Uncertainty to be less than 10 km<sup>-1</sup> had the largest impacts on reducing the difference  
237 in mean and medians of the AERONET and CATS AOD. Still, this exercise highlights the need  
238 for careful quality checks of the CATS data before applying the CATS data for advanced  
239 applications to overcome cloud-aerosol discrimination uncertainties.

240

### 241 3.1.2 CATS-MODIS

242 To examine over ocean performance, column integrated CATS AODs are inter-compared  
243 with collocated Terra and Aqua C6.1 MODIS DT over ocean AOD, interpolated to 1064 nm. Over  
244 ocean C6.1 MODIS DT data are selected due to the fact that higher accuracies are reported for  
245 over ocean versus over land MODIS DT AOD retrievals (Levy et al., 2013). In addition, comparing  
246 with over land MODIS DT data, which provides AOD retrievals at three discrete wavelengths  
247 (0.46, 0.55 and 0.65  $\mu\text{m}$ ), over water AOD retrievals are available from 7 wavelengths including  
248 the 0.87 and 1.24  $\mu\text{m}$  spectral channels, allowing a comparison with CATS AOD at the same

Moved (insertion) [3]

Deleted: 17

Deleted: T

Deleted: Note that similar results are found in comparisons between collocated CATS and MODIS/CALIPSO data without the use of QA procedures on CATS data.

Moved up [3]: Thus, only QAed CATS data are used hereafter.

255 wavelength upon logarithmic interpolation, again, assuming the aerosol Ångström Exponent value  
256 remains unchanged from 0.87 to 1.064  $\mu\text{m}$  as well as from 1.064  $\mu\text{m}$  to 1.24  $\mu\text{m}$  spectral channels.

257 MODIS and CATS AOT retrievals are collocated for the study period of Feb. 2015-Oct.  
258 2017 (Figure 2). Pairs of CATS and MODIS data were first selected for both retrievals that fall  
259 within  $\pm 30$  minutes and 0.4 degrees latitude and longitude of each other. Then, similar to the  
260 AERONET and CATS collocation procedures, collocated pairs were further averaged to construct  
261 one pair of collocated MODIS and CATS data for a given collocation incident. Shown in Figure  
262 2a, a correlation of 0.72 is found between collocated over water Terra MODIS C6.1 DT and CATS  
263 AODs with a slope of 0.74. Similar results are found for the comparisons between over water  
264 Aqua MODIS and CATS AODs with a correlation of 0.74 and a slope of 0.70.

### 266 3.1.3 CATS-CALIOP AOD

267 In the previous two sections, AODs from CATS are inter-compared with retrievals from  
268 passive-based sensors such as MODIS and AERONET. In this section, AOD data from CALIOP,  
269 which is an active sensor, are evaluated against AOD retrievals from CATS. Note that despite  
270 difference in instrumental designs, CALIOP and CATS are both elastic backscatter lidars. Again,  
271 for each collocation incident, pairs of CALIOP and CATS data are selected in which both retrievals  
272 fall within  $\pm 30$  minutes temporally and 0.4 degrees latitude and longitude spatially. There could  
273 be multiple CATS retrievals corresponding to one CALIOP data point, and vice versa. Thus, the  
274 collocated pairs are further averaged in such a way that only one pair of collocated CATS and  
275 CALIOP data is derived for each collocation incident. \*

276 Figure 3a shows the comparison of CATS and CALIOP AODs for all collocated pairs  
277 including both day- and night-time. A reasonable correlation of 0.74, with a slope of 0.73, is found

**Formatted:** Font: (Default) Times New Roman, 12 pt, Not Italic

**Moved up [2]:** Mean and standard deviation of Ångström exponents using this method were 0.69 and 0.55, respectively.

**Formatted:** Font: (Default) Times New Roman, 12 pt

**Formatted:** Font: (Default) Times New Roman, 12 pt, Not Italic

**Formatted:** Font: (Default) Times New Roman, 12 pt

**Formatted:** Font: (Default) Times New Roman, 12 pt, Not Italic

**Formatted:** Font: (Default) Times New Roman, 12 pt, Not Italic

**Formatted:** Font: (Default) Times New Roman, 12 pt, Not Italic

**Moved down [1]:** Note that as suggested by Omar et al., (2013), the choices of spatial and temporal collocation windows have an effect on collocation results.

**Deleted:** However, we consider this as a topic beyond the scope of this study

285 for a total of 2762 collocated data pairs. Further breaking down the comparison into day and night  
286 cases, a much better agreement is found between the two datasets during nighttime with  
287 correlations of 0.81 and 0.83 for over-ocean and over-land cases respectively. In comparison, a  
288 lower correlation of 0.64, with a slope of 0.49, is found between the two datasets, using over land  
289 daytime data only, for a total of 170 collocated pairs. Correspondingly, a lower correlation of  
290 0.55, with a slope of 0.57, is found between the two datasets, using over ocean daytime data only,  
291 for a total of 1180 collocated pairs. This result is not surprising as daytime data from both CALIOP  
292 and CATS are noisier due to solar contamination (e.g. Omar et al., 2013; Toth et al., 2016).

293 Note that based on the slopes of the regression lines shown in Figures 1-3, AODs retrieved  
294 by CATS are less than AERONET, CALIOP and DT Aqua MODIS AOD retrievals. As shown  
295 in Table 1, however, for the one-to-one collocated datasets, mean CATS AODs (1064 nm) are  
296 ~10% higher than AERONET AODs (1020 nm). The CATS AODs are ~3% higher than CALIOP  
297 AOD (1064 nm) and are ~5-10% higher than DT MODIS AODs. One possible explanation for  
298 this discrepancy is because mean AODs are dominated by low AOD cases and the slopes of the  
299 regression relationships are strongly affected by a few high AOD cases. Thus, it is likely that  
300 CATS AODs are overestimated at the low AOD ranges and are underestimated at the high AOD  
301 ranges.

302 Also note that as suggested by Omar et al., (2013), the choices of spatial and temporal  
303 collocation windows have an effect on collocation results. Thus, we repeated the exercises in Figures  
304 1-3 by doubling the spatial and temporal collocation windows as well as reducing the collocation  
305 windows by half. The descriptive statistics of this sensitivity study is included in Table 2. While  
306 the number of collocated data pairs are drastically affected by the spatial and temporal collocation  
307 window sizes, less significant changes, however, are found in descriptive statistics such as mean.

Moved (insertion) [1]

Deleted: N

309 median, and standard deviations of AODs, as well as slopes and correlation values. The slope of  
310 DT Aqua MODIS and CATS AODs, however, seems sensitive to changes in collocation methods.  
311 Changes in slope of 0.61 to 0.78 are found for the change of temporal collocation window from  
312 15 minutes to 60 minutes with a fixed spatial collocation window of 0.4° Latitude/Longitude.

313 Still, larger discrepancies between CATS and CALIOP AODs during daytime indicate that  
314 both sensors are susceptible to solar contamination. To overcome solar contamination and more  
315 accurately detect aerosol layers, CALIOP and CATS data products are averaged up to 80 km and  
316 60 km, respectively. Noel et al. (2018) found that the feature type score can be used for clouds  
317 screening throughout the diurnal envelope of solar angles. To further evaluate impact of the solar  
318 contamination introduced bias in the diurnal analysis in aerosol detection or products, CATS  
319 AODs are evaluated as a function of local time. For each CATS observation of a given location  
320 and UTC time, the associated local time is computed by adding the UTC time by 1 hour per 15°  
321 Longitude away from the Prime Meridian in the east direction. Figure 4a shows the CATS AOD  
322 versus local time for both global land and oceans, constructed using 6 hourly mean CATS AOD  
323 binned on a 5 degree by 5 degree grid globally. While the data has additional noise, no major  
324 deviations in AODs are found during either sunrise or sunset time, although we speculate that  
325 larger uncertainties in CATS AODs and extinctions may be present around day and night  
326 terminators. Figure 4b shows a similar plot as Figure 4a, but with the region restricted to 25°S-  
327 52°S. Here, we want to investigate the variations in CATS AODs as a function of local time, over  
328 relatively aerosol free oceans. We picked 25°S as the cutoff line as CATS data only available to  
329 51.6°S (limited to the ISS inclination angle) and thus, this threshold is used to ensure enough data  
330 samples in the analysis, although some land regions are also included. As indicated in Figure 4b,  
331 again, no significant deviations in pattern are found for both sunrise and sunset time, plausibly

332 indicating that solar contamination, as speculated, may not be as significant. Comparing the mean  
333 AOD at local midnight to the mean AOD at local noon by performing a student's t test, the  
334 difference is not significant at the 95% confidence level, with a p-value of 0.16.

335 Figure 4c shows the difference between AERONET (1020 nm) and CATS (1064 nm) AOD  
336 ( $\Delta$ AOD) as a function of local time, again, although data are rather noisy, no major pattern is found  
337 near sunrise or sunset times, again, further indicating that solar contamination during dawn or dusk  
338 times, may have a less severe impact to CATS AOD retrievals from a long term mean perspective.

339 In summary, Sections 3.1.1-3.1.3 suggest that with careful QA procedures, AOD retrievals from  
340 CATS are comparable to those from other existing sensors such as AERONET, MODIS, and  
341 CALIOP at the same local times.

#### 343 3.1.4 CATS-CALIOP Vertical Extinction Profiles

344 One advantage of CATS is its ability to retrieve both column-integrated AOD and vertical  
345 distributions of aerosol extinction. Therefore, in this section, extinction profiles from CATS are  
346 compared with that from CALIOP. Again, similar to the Section 3.1.3, collocated profiles for  
347 CATS and CALIOP are first found for both retrievals that are close in space and time (within  $\pm 30$   
348 minutes and 0.4 degrees latitude and longitude). However, different from Section 3.1.3, only one  
349 pair of collocated CATS and CALIOP profiles, which has the closest Euclidian distance on the  
350 earth's surface, is retained for each collocated incident.

351 The CATS cloud-aerosol discrimination (CAD) algorithm is a multidimensional  
352 probability density function (PDF) technique that is based on the CALIPSO algorithm (Liu et al.  
353 2009). The PDFs were developed based on Cloud Physics Lidar (CPL) measurements obtained  
354 during over 11 field campaigns and 10 years. As shown in Figure 5e, a reasonable agreement is

355 found between CATS V3-00 aerosol extinction with CALIOP for over land. However, CATS  
356 overestimates aerosol extinction around 1 km compared to CALIOP over ocean (Figure 5d). This  
357 can also be seen on a plot of the difference between CATS and CALIOP 1064 nm extinction for  
358 all collocated profiles, included in Figure 5f, where there is an overall positive difference around  
359 1 km.

360 Due to the precessing orbit of the ISS, the CATS sampling is irregular and very different  
361 compared to the sun-synchronous orbits of the A-Train sensors. These orbital differences between  
362 CATS and CALIOP make comparing the data from these two sensors challenging since they are  
363 fundamentally observing different locations of the Earth at different times. Thus, we shouldn't  
364 expect the extinction profiles and AOD from these two sensors to completely agree. Additionally,  
365 there are other algorithm and instrument differences that can lead to differences in extinction  
366 coefficients and AOD. Over land where dust is the dominant aerosol type, differences in lidar  
367 ratios between the two retrieval algorithms (CATS uses 40 sr while CALIOP uses 44 sr), can cause  
368 CATS extinction coefficients that are up to 10% lower than CALIOP, potentially explaining the  
369 higher CALIOP extinction values in Figure 5e. Over ocean, especially during daytime, differences  
370 in CATS and CALIOP lidar ratios for marine and smoke aerosols can introduce a difference  
371 between CATS and CALIOP extinction coefficients (Figure 5d). These difference in over ocean  
372 data (Figure 5d) could also attributed to differences in CATS and CALIOP 1064 nm backscatter  
373 calibration. For example, Pauly et al. (2019) reports that CATS attenuated total backscatter is  
374 about 19.7% lower than PollyXT measurements in the free troposphere and 19% lower than  
375 CALIOP of opaque cirrus clouds due to calibration uncertainties for both sensors.

376 Also, differences in the lowest 250 m between CATS and CALIOP extinction profiles are  
377 observable, which are due to how the instrument algorithms detect the surface and near-surface

378 aerosols. Both the CATS and CALIOP feature detection algorithms create a gap between the  
379 surface and near-surface aerosol base altitude, despite the possible presence of aerosols in this  
380 altitude region. CALIOP has an aerosol base extension algorithm that is designed to (1) detect  
381 scenarios when aerosols are present in the bins just above the surface and (2) extend the near-  
382 surface aerosol layer base down to the surface (Tackett et al., 2018). However, CATS does not use  
383 such an algorithm so false regions of “clear-air” exist between the surface and near-surface aerosol  
384 layers.

385 Vertical profiles of collocated CATS and CALIOP extinction for daytime only profiles and  
386 nighttime only profiles are shown in Figure 5b and 5c, respectively. Compared to a total collocated  
387 pair count of 2681 in the overall profile data, day and night profiles have 1311 and 1437 collocated  
388 pairs, respectively. Again, the shapes of the CATS and the CALIOP nm extinction vertical profile  
389 are similar for all three cases, despite the above mentioned offsets in altitude. Figure 5d and 5e  
390 show the mean of those extinction profiles which occurred over-water and over-land, as defined  
391 by the CATS surface type flag. Again in both cases CATS and CALIOP have similar shapes in  
392 their vertical extinction profiles. The vertical structure of over-water extinction is also very similar  
393 to that of all profiles, day, and night, which is perhaps not surprising as water profiles made up  
394 2142 of 2748 (~78%) collocated pairs. The vertical structure of over-land is more different than  
395 the other groups, as the extinction is higher throughout a larger depth of the atmosphere, tapering  
396 off much more slowly from the surface. Furthermore, the extinction from CATS is actually lower  
397 than CALIOP for over-land profiles, unlike all other categories.

### 398

### 399 **3.2 Diurnal Cycle of AODs and Aerosol Vertical Distributions**

400 Using the QAed CATS data, seasonal variations as well as diurnal variations in CATS  
401 AODs are derived in this section. Diurnal variations in the vertical distributions of CATS aerosol  
402 extinction are also examined at both global and regional scales.

403

### 404 **3.2.1 Seasonal and Diurnal Variation of AOD**

405 Figures 6a-b show the spatial distributions of CATS AODs at the 1064 nm spectral channel  
406 for boreal winter-spring (Dec.-May, DJFMAM) and boreal summer-fall (June-Nov, JJASON)  
407 seasons, for the period of Feb. 2015-Oct. 2017. To construct Figures 6a and 6b, quality-assured  
408 CATS AODs are first binned on a 5 degree by 5 degree grid over the globe for the above mentioned  
409 two bi-seasons. For each  $5 \times 5^\circ$  (Latitude/Longitude) bin, for a given season, CATS AODs are  
410 averaged on a pass-basis first, and then further averaged seasonally to represent AOD value of the  
411 given bin. [Both daytime and nighttime retrievals are included in this Figure, as well as Figures 7-](#)  
412 [9.](#)

413 In DJFMAM season, significant aerosol features are found over North Africa, Mid-East,  
414 India and Eastern China. For the JJASON season, besides the above mentioned regions, aerosol  
415 plumes are also observable over Southern Africa, related to summer biomass burning of the region  
416 (e.g. Eck et al., 2013). The seasonal-based spatial distributions of AODs from CATS, although  
417 reported at the 1064 nm channel [that](#) is different from the 550 nm channel that is conventionally  
418 used, are similar to some published results (e.g. Lynch et al., 2016).

419 For comparison purposes, Figures 6c-6d shows similar plots as Figures 6a-6b, but with the  
420 use of CALIOP AOD at the 1064 nm spectral channel. Note that those are climatological means  
421 rather than pairwise comparisons. While patterns are similar in general, at regions with peak  
422 AODs of 0.4 or above for CALIOP, such as North Africa for the DJFMAM season and North

423 Africa, Middle-East and India for the JJASON, much lower AODs are found for CATS. In some  
424 other regions, such as over South Africa for the JJASON season, however, higher CATS AOD  
425 values are observed. A table of mean AOD across each of these regions as well as over the globe  
426 (within the latitude range where CATS has data) has been included for reference (Tables 3).  
427 Figures 6e and 6f show the similar spatial plots as Figures 6a and 6b but with the use of Aqua  
428 MODIS AODs from the DT products (using all available MODIS DT retrievals that passed QA  
429 steps as described in Section 2.3). For the Aqua MODIS DT products, aerosol retrievals at the  
430 short-wave Infra-red channels are only available over oceans, and thus Figures 6e-6f show only  
431 over ocean retrievals. Again, while general AOD patterns look similar, discrepancies are also  
432 visible, such as over the coast of south east Africa for the JJASON season and over the west coast  
433 of Africa for the DJFMAM season. Those discrepancies may result from biases in each product,  
434 but it is also possibly due to the differences in satellite overpass times, as CALIOP provides early  
435 morning and afternoon over passes, and Aqua MODIS has an over pass time after local noon,  
436 while CATS is able to report atmospheric aerosol distributions at multiple times during a day.

437 Similar to Figures 6a and 6b, Figures 7a and 7b show the spatial distribution of CATS  
438 AODs, but for CATS extinction values that are below 1 km Above Ground Level (AGL) only, for  
439 the DJFMAM and JJASON seasons respectively. Figure 7c and 7d (7e and 7f) show the CATS  
440 mean AOD plots for extinction values from 1-2 km AGL (> 2 km AGL). For the DJFMAM  
441 season, elevated aerosol plumes with altitude above 2 km AGL are found over the North Africa.  
442 For the JJASON season, elevated dust plumes (> 2 km AGL) are found over North Africa and the  
443 Middle-East regions, while elevated smoke plumes are found over the west coast of South Africa  
444 where above cloud smoke plumes are often observed during the Northern hemispheric summer  
445 season (e.g. Alfaro-Contreras et al., 2016).

446 CATS has a non-sun-synchronized orbit, which enables measurements at nearly all solar  
447 angles. Thus, we also constructed  $5 \times 5^\circ$  (Latitude/Longitude) gridded seasonal averages (for  
448 DJFMAM and JJASON seasons) of CATS AODs at 0, 6, 12 and 18 UTC that represent 4 distinct  
449 times in a full diurnal cycle, as shown in Figure 8. To construct the seasonal averages, observations  
450 within  $\pm 3$  hours of a given UTC time as mentioned above are averaged to represent AODs for the  
451 given UTC time. On a global average, the mean AODs are 0.090, 0.089, 0.088 and 0.089 for 0, 6,  
452 12 and 18 UTC respectively for the JJASON season and are 0.099, 0.096, 0.093 and 0.093 for the  
453 DJFMAM season. Thus, no significant diurnal variations are found on a global scale.

454 Still, strong diurnal variations with the maximum averaged diurnal AOD changes of above  
455 0.10 can be observed for regions with significant aerosol events such as Northern Africa, Mid-East  
456 and India for the DJFMAM season and Northern Africa, Southern Africa, Mid-East and India for  
457 the JJASON season, as illustrated in Figure 9. Note that Fig. 9a shows the maximum minus  
458 minimum seasonal mean AODs for the four difference times as shown in Figs. 8a,c,e,g. Similarly,  
459 Fig. 9b shows the maximum minus minimum seasonal mean AODs for the four difference times  
460 as shown in Figs. 8b,d,f,h. Interestingly but not unexpectedly, regions with maximum diurnal  
461 variations match well with locations of heavy aerosol plumes as shown in Figures 6 and 8.

### 462

### 463 **3.2.2 Diurnal variations of Aerosol Extinction on a Global Scale (both at UTC and local time)**

464 Using quality-assured CATS derived aerosol vertical distributions, mean global CATS  
465 extinction vertical profiles are also generated as shown in Figure 10. Similar to steps as described  
466 in the section 3.2.1, CATS extinction profiles are binned into 00, 06, 12, and 18 UTC times based  
467 on the closest match in time for the JJASON and DJFMAM seasons. Figure 10a shows the daily  
468 averaged CATS extinction profiles in a black line, and 00, 06, 12 and 18 UTC averaged in blue,

469 green, yellow and red lines respectively, for the DJFMAM season. [Similar plot is shown in Figure](#)  
470 [10d for the JJASON season.](#) CATS extinction profiles for the daily average as well averages for  
471 the four selected times are similar, suggesting that minor temporal variations in CATS extinctions  
472 can be expected for global averages.

473 Those global averages are dominated by CATS profiles from global oceans (Figure 10b  
474 and 10e), which also have small diurnal variations, as ~70% of the globe is covered by water. In  
475 comparison, noticeable diurnal changes in aerosol vertical distributions are found over land as  
476 shown in Figure 10c and 10f. For the DJFMAM season, at the 1 km altitude, the minimum and  
477 maximum aerosol extinctions are at 12 and 18 UTC respectively. Similarly, the minimum and  
478 maximum aerosol extinctions are at 12 and 00 UTC at the altitude of 400 m. For the JJASON  
479 season, the minimum aerosol extinction values are found at 12 UTC for the whole 0-2 km column,  
480 while the maximum aerosol extinction values are at 18UTC for 1.5 km and 00 UTC for the 300-  
481 400 m altitude. Still, it should be noted that aerosol concentrations may be a function of local  
482 time, yet for a given UTC time, local times will vary by region. Also, due to solar contamination,  
483 nighttime retrievals from CATS are significantly and demonstrably less noisy than daytime retrievals,  
484 and this difference in sensor sensitivity between day and night may further affect the derived  
485 diurnal variations in CATS AOD and aerosol vertical profiles as shown in Figure 3 for individual  
486 retrievals. Still, no apparent solar pattern is detectable from Figure 8, and only minor diurnal  
487 variations are found for Figure 10a and 10d, which indicate that such a solar contamination may  
488 introduce noise but not bias to daytime aerosol retrievals, from a global mean perspective.

489 If we examine the mean global CATS extinction vertical profiles with respect to local time  
490 as shown in Figure 11, however, some distinct features appear. For example, Figure 11a and 11d  
491 suggests that on global average, the minimum aerosol extinction below 1 km is found for 6:00 pm

492 local time, for both JJASON and DJFMAM seasons. Similar patterns are also observed for over  
493 global oceans. However, for over land cases, for both seasons, the minimum and maximum aerosol  
494 extinction below 600 m is found for 12:00 pm and 00:00/06:00 am local time.  
495

### 496 **3.2.3 Diurnal variations of Aerosol Extinction on a Regional Scale (at local time)**

497 In this section, the diurnal variations of aerosol vertical distributions are studied as a  
498 function of local solar time for selected regions with high mean AODs as highlighted in Figure 6.  
499 We picked local solar time here as for those regional analyses. Note a near 1 to 1 transformation  
500 can be achieved between UTC and local solar time. Also, as learned from the previous section,  
501 aerosol features are likely to have a local time dependency. A total of four regions, including  
502 Africa-north, Middle East, India and Northeast China, which show significant seasonal mean  
503 AODs in Figure 6, are selected for the DJFMAM season (Figure 12). For the JJASON season  
504 (Figure 13), in addition to the above mentioned 4 regions, the Africa-south region is also included  
505 due to biomass burning in the region during the Northern Hemisphere summer time. The  
506 Latitude/Longitude boundary of each selected region is described in Table 4. Regional-based  
507 analyses are also conducted for 4 selected regions for the DJFMAM season and 5 selected regions  
508 for the JJASON season at four local times: 0:00 am (midnight), 6:00 am, 12:00 pm and 6:00 pm,  
509 using quality assured CATS profiles. Generally, the maximum diurnal change in aerosol  
510 extinction is found at the altitude of below 1 km for all regions as well for both seasons. Also,  
511 larger diurnal variations in vertical distributions of aerosol extinction are found for the JJASON  
512 season, in-comparing with the DJFMAM season, while regional-based differences are apparent.

513 For the Africa-north region, dominant aerosol types are dust and smoke aerosol for the  
514 DJFMAM season, and is dust for the JJASON season (e.g. Remer et al., 2008). Interestingly, the

515 maximum aerosol extinction below 500m is found at 6:00 am for the DJFMAM season. While for  
516 the JJASON season, the maximum aerosol extinctions are found at 0:00 am / 6:00 am for the 100-  
517 500 m layer, with a significant ~10-20% higher aerosol extinction from the daily mean. Note that  
518 6:00 am in the Africa-north region corresponds to early morning, which has been identified in  
519 several studies (Fiedler et al., 2013; Ryder et al. 2015) as the time of day when nocturnal low-level  
520 jet breakdown causes large amounts of dust emission in this region. Thus, we suspect that this  
521 6:00 am peak in maximum aerosol extinctions may be the signal resulting from the low-level jet  
522 ejection mechanism captured on a regional scale. As the day progresses into the afternoon and  
523 early evening, we find the aerosol heights shifting upwards, likely related to the boundary layer's  
524 mixed layer development.

525 For the Middle East region, for the JJASON season, a daily maximum in aerosol extinction  
526 of ~0.15  $\text{km}^{-1}$  is found at midnight (0:00 am) , with a daily minimum of ~0.08  $\text{km}^{-1}$  found at local  
527 noon (12:00 pm), for the peak aerosol extinction layer that has a daily mean aerosol extinction of  
528 ~0.12  $\text{km}^{-1}$ . This translates to a ~±20-30% daily variation for aerosol extinction for the peak  
529 aerosol extinction layer. Smaller daily variation in aerosol extinction, however, is found for the  
530 same region for the DJFMAM season.

531 For the India region, for the JJASON season, a large peak in aerosol extinction of up to  
532 10% higher than daily mean is found at 6:00 am below 500 m. The minimum aerosol extinction  
533 is found at 12:00/6:00 pm for the layer below 500 m, and is overall ~10% lower than the peak  
534 daily mean aerosol extinction value. For the DJFMAM season, minimum aerosol extinctions are  
535 found at 12:00 pm for near the whole 0-2 km column, while for the layer below 500 m, the  
536 maximum aerosol extinction values are found at mid-night (0:00 am).

537 For the Northeast China region , a significant peak found at the 500m-1km layer for local  
538 afternoon (6:00 pm) for the DJFMAM season. A similar feather is also found for the JJASON  
539 season. While the peak extinction for the JJASON season happens at 06:00am for the aerosol  
540 layer below 500m. Lastly, for the Africa-south region, biomass burning aerosols are prevalent  
541 during the summer time and thus only the JJASON season is analyzed. As shown in 13b, below  
542 500m in altitude, lower extinction values are found for local afternoon (18:00 pm) and higher  
543 extinction values are found for local morning or early morning (0:00 and 6:00 am).

#### 545 **4.0 Conclusions**

546 Using CALIOP, MODIS and AERONET data, we evaluated CATS derived AODs as well  
547 as vertical distributions of aerosol extinctions for the study period of for Feb. 2015 – Oct. 2017.  
548 CATS data (at 1064 nm) are further used to study variations in AODs and aerosol vertical  
549 distributions diurnally. We found:

550 (1) Quality assurance steps are critical for applying CATS data in aerosol related  
551 applications. With a less than 2% data loss due to QA steps, an improvement in  
552 correlation from 0.51 to 0.65 is found for the collocated CATS and AERONET AOD  
553 comparisons. Using quality assured CATS data, reasonable agreements are found  
554 between CATS derived AODs and AODs from CALIOP, Aqua MODIS DT and Terra  
555 MODIS DT at the same local times, with correlations of 0.74, 0.74 and 0.72  
556 respectively.

557 (2) While the averaged vertical distributions from CATS compare reasonably well with  
558 that from CALIOP, differences in peak extinction altitudes are present. This may due

559 to sampling difference as well as algorithm and instrument differences such as different  
560 lidar ratios used.

561 (3) From the global mean perspective, minor changes are found for AODs at four selected  
562 times, namely 00, 06, 12 and 18 UTC. Yet noticeable diurnal variations in AODs of  
563 above 0.10 (at 1064 nm) are found for regions with extensive aerosol events, such as  
564 over North Africa, Middle East, and India for the DJFMAM season, and over North  
565 and South of Africa, India and Middle East for the JJASON season.

566 (4) From the global mean perspective, changes are less noticeable for the averaged aerosol  
567 extinction profiles at 00, 06, 12 and 18 UTC. Yet, if the study is repeated with respect  
568 to local time, a peak in aerosol extinction is found for local noon (12:00pm) for the  
569 DJFMAM season and the minimum value in aerosol extinction is found at 6:00 pm  
570 local time for both JJASON and DJFMAM seasons. While the over water aerosol  
571 vertical distributions are similar to the global means, for over land cases, the minimum  
572 and maximum extinctions are found at local noon (12:00pm) and local morning or early  
573 morning (6:00am and 0:00am) for the layer below 500 m for both seasons.

574 (5) Larger diurnal variations are found at regions with heavy aerosol plumes such as North  
575 and South (summer season only) of Africa, Middle East, India and Eastern China. In  
576 particular, aerosol extinctions from 6:00 am over North Africa are ~10% higher than  
577 daily means for the 0-500 m column for both seasons. We suspect this may be related  
578 to increase in dust concentrations due to breakdown of low level jets at early morning  
579 time for the region.

580 (6) Still, readers shall be aware that AOD retrievals at the 1064 nm are less sensitive to  
581 fine mode aerosols such as smoke and pollutant aerosols, compared to coarse mode

582 aerosols such as dust aerosols [\(e.g. Dubovik et al., 2000\)](#). Thus, an investigation of  
583 diurnal variations of aerosol properties at the visible channel may be also needed for a  
584 future study.

585 This paper suggests that strong regional diurnal variations exist for both AOD and aerosol  
586 extinction profiles. Still, at present these conclusions are tentative, and will remain so until a  
587 comprehensive analysis of the CATS calibration accuracy and stability is completed. These results  
588 demonstrate the need for global aerosol measurements throughout the entire diurnal cycle to  
589 improve visibility and particulate matter forecasts as well as studies focused on aerosol climate  
590 applications.

591  
592 **Author Contribution:**

593 Authors J. Zhang, J. S. Reid and L. Lee designed the study. L. lee worked on data processing for  
594 the project. J. E. Yorks guided L. lee on data processing. The manuscript was written with inputs  
595 from all coauthors.

596 **Acknowledgments:**

597 We acknowledge the support of ONR grant (N00014-16-1-2040) and NASA grant  
598 (NNX17AG52G) for this study. L. Lee is also partially supported by the NASA NESSF  
599 fellowship grant (NNX16A066H). J. S Reid's participation was supported by the Office of Naval  
600 Research Code 322 and 33. We thank the NASA AERONET team for the AERONET data used  
601 in this study.

603 **References:**

604 Aerosol Product Application Team of the AWG Aerosols/Air Quality/Atmospheric Chemistry  
605 Team: GOES-R Advanced Baseline Imager (ABI) algorithm theoretical basis document  
606 for suspended matter/aerosol optical depth and aerosol size parameter,  
607 NOAA/NESDIS/STAR July 2012,  
608 <https://www.star.nesdis.noaa.gov/goesr/docs/ATBD/AOD.pdf> (last accessed on Nov. 17,  
609 2018).

610 Alfaro-Contreras, R., Zhang, J., Campbell, J. R., and Reid, J. S.: Investigating the frequency  
611 and trends in global above-cloud aerosol characteristics with CALIOP and OMI, *Atmos.*  
612 *Chem. Phys.*, 16, 47-69, doi:10.5194/acp-16-47-2016, 2016.

613 Campbell, J. R., Tackett, J. L., Reid, J. S., Zhang, J., Curtis, C. A., Hyer, E. J., Sessions, W.  
614 R., Westphal, D. L., Prospero, J. M., Welton, E. J., Omar, A. H., Vaughan, M. A., and  
615 Winker, D. M.: Evaluating nighttime CALIOP 0.532  $\mu\text{m}$  aerosol optical depth and  
616 extinction coefficient retrievals, *Atmos. Meas. Tech.*, 5, 2143-2160,  
617 <https://doi.org/10.5194/amt-5-2143-2012>, 2012.

618 CATS Algorithm Theoretical Basis Document:  
619 [https://cats.gsfc.nasa.gov/media/docs/CATS\\_ATBD\\_V1-02.pdf](https://cats.gsfc.nasa.gov/media/docs/CATS_ATBD_V1-02.pdf), 2016; accessed on March  
620 28, 2019.

621 Christopher, S. A. and Zhang, J.: Daytime variation of shortwave direct radiative forcing of  
622 biomass burning aerosols from GOES 8 imager, *J. Atmos. Sci.*, 59, 681–691, 2002.

623 [Dubovik, O., Smirnov, A., Holben, B. N., King, M. D., Kaufman, Y. J., Eck, T. F., and](#)  
624 [Slutsker, I.: Accuracy Assessments of Aerosol Optical Properties Retrieved from Aerosol](#)

625 [Robotic Network \(AERONET\) Sun and Sky Radiance Measurements, J. Geophys. Res.-](#)  
626 [Atmos., 105, 9791–9806, <https://doi.org/10.1029/2000JD900040>, 2000.](#)

627 Eck, T. F., Holben, B. N., Reid, J. S., Mukelabai, M. M., Piketh, S. J., Torres, O., Jethva, H.  
628 T., Hyer, E. J., Ward, D. E., Dubovik, O., and Sinyuk, A.: A seasonal trend of single  
629 scattering albedo in southern African biomass-burning particles: Implications for satellite  
630 products and estimates of emissions for the world’s largest biomass-burning source, J.  
631 Geophys. Res.-Atmos., 118, 6414–6432, 2013.

632 Fiedler, S., Schepanski, K., Heinold, B., Knippertz, P., and Tegen, I.: Climatology of  
633 nocturnal low-level jets over North Africa and implications for modeling mineral dust  
634 emission, J. Geophys. Res. Atmos., 118, 6100–6121, doi: 10.1002/jgrd.50394, 2013.

635 Giglio, L., Kendall, J.D., Mack, R.: A multi-year active fire dataset for the tropics derived from  
636 the TRMM VIRS., International Journal of Remote Sensing 24, 4505-4525, 2003.

637 [Giles, D. M., Sinyuk, A., Sorokin, M. G., Schafer, J. S., Smirnov, A., Slutsker, I., Eck, T. F.,](#)  
638 [Holben, B. N., Lewis, J. R., Campbell, J. R., Welton, E. J., Korkin, S. V., and Lyapustin,](#)  
639 [A. I.: Advancements in the Aerosol Robotic Network \(AERONET\) Version 3 database –](#)  
640 [automated near-real-time quality control algorithm with improved cloud screening for Sun](#)  
641 [photometer aerosol optical depth \(AOD\) measurements, Atmos. Meas. Tech., 12, 169-209,](#)  
642 <https://doi.org/10.5194/amt-12-169-2019>, 2019.

643 Heinold, B., Knippertz, P., Marsham, J. H., Fiedler, S., Dixon, N. S., Schepanski, K., Laurent,  
644 B., and Tegen, I.: The role of deep convection and nocturnal low-level jets for dust  
645 emission in summertime West Africa: Estimates from convection-permitting  
646 simulations, J. Geophys. Res. Atmos., 118, 4385–4400, doi:10.1002/jgrd.50402, 2013.

647 Holben, B. N., and coauthors: AERONET—A Federated Instrument Network and Data  
648 Archive for Aerosol Characterization. *Remote Sensing of Environment*, 66(1), 1–16.  
649 [https://doi.org/10.1016/S0034-4257\(98\)00031-5](https://doi.org/10.1016/S0034-4257(98)00031-5), 1998.

650 Hyer, E. J., Reid, J. S., Prins, E. M., Hoffman, J. P., Schmidt, C. C., Miettinen, J. I., and Giglio,  
651 L.: Different views of fire activity over Indonesia and Malaysia from polar and  
652 geostationary satellite observations, *Atmos. Res.*, 122, 504-519, 2013.

653 Kaku K. C., Reid, J. S., Hand, J. L., Edgerton, E. S., Holben, B. N., Zhang, J., and Holz, R. E.:  
654 Assessing the challenges of surface-level aerosol mass estimates from remote sensing  
655 during the SEAC4RS campaign: Baseline surface observations and remote sensing in the  
656 Southeastern United States, *JGR*, doi: 10.1029/2017JD028074, 2018.

657 Levy, R. C., Mattoo, S., Munchak, L. A., Remer, L. A., Sayer, A. M., Patadia, F., and Hsu, N.  
658 C.: The Collection 6 MODIS aerosol products over land and ocean. *Atmos. Meas. Tech.*,  
659 6(11), 2989–3034. <https://doi.org/10.5194/amt-6-2989-2013>, 2013.

660 Liu, Z., and coauthors: The CALIPSO Lidar Cloud and Aerosol Discrimination: Version 2  
661 Algorithm and Initial Assessment of Performance, *J. Atmos. Oceanic Technol.*, 26, 1198–  
662 1213, 2009.

663 Lynch, P., Reid, J. S., Westphal, D. L., Zhang, J., Hogan, T. F., Hyer, E. J., Curtis, C. A., Hegg,  
664 D. A., Shi, Y., Campbell, J. R., Rubin, J. I., Sessions, W. R., Turk, F. J., and Walker, A.  
665 L.: An 11-year global gridded aerosol optical thickness reanalysis (v1.0) for atmospheric  
666 and climate sciences, *Geosci. Model Dev.*, 9, 1489-1522, [https://doi.org/10.5194/gmd-9-](https://doi.org/10.5194/gmd-9-1489-2016)  
667 1489-2016, 2016.

668 Mbourou, G. N., Berand, J. J., and Nicholson, S. E.: The diurnal and seasonal cycle of wind-  
669 borne dust over Africa north of the equator, *J. Appl. Meteor.*, 36, 868-882, 1997.

670 McGill, M. J., Yorks, J. E., Scott, V. S., Kupchock, A. W., and Selmer, P. A.: The Cloud-  
671 Aerosol Transport System (CATS): A technology demonstration on the International Space  
672 Station, Proc. SPIE 9612, Lidar Remote Sensing for Environmental Monitoring XV,  
673 96120A, doi:10.1117/12.2190841, 2015.

674 Noel, V., Chepfer, H., Chiriaco, M., and Yorks J. E.: The diurnal cycle of cloud profiles over  
675 land and ocean between 51° S and 51° N, seen by the CATS spaceborne lidar from the  
676 International Space Station, Atmos. Chem. Phys., 18, 9457-9473,  
677 <https://doi.org/10.5194/acp-18-9457-2018>, 2018.

678 Omar, A. H., Winker, D. M., Tackett, J. L., Giles, D. M., Kar, J., Liu, Z., Vaughan, M. A.,  
679 Powell, K. A., and Trepte C. R.: CALIOP and AERONET aerosol optical depth  
680 comparisons: One size fits none, J. Geophys. Res. Atmos., 118, 4748–4766, doi:  
681 10.1002/jgrd.50330, 2013.

682 [Pauly, R. M., Yorks, J. E., Hlavka, D. L., McGill, M. J., Amiridis, V., Palm, S. P., Rodier, S.](#)  
683 [D., Vaughan, M. A., Selmer, P. A., Kupchock, A. W., Baars, H., and Gialitaki, A.: Cloud](#)  
684 [Aerosol Transport System \(CATS\) 1064 nm Calibration and Validation, Atmos. Meas.](#)  
685 [Tech. Discuss., <https://doi.org/10.5194/amt-2019-172>, in review, 2019.](#)

686 Rajapakshe, C., Zhang, Z., Yorks, J. E., Yu, H., Tan, Q., Meyer, K., Platnick, S.: Seasonally  
687 Transported Aerosol Layers over Southeast Atlantic are Closer to Underlying Clouds than  
688 Previously Reported, Geophys. Res. Lett., 44, doi:10.1002/2017GL073559, 2017.

689 Redemann, J., Vaughan, M. A., Zhang, Q., Shinozuka, Y., Russell, P. B., Livingston, J. M., ...  
690 Remer, L. A.: The comparison of MODIS-Aqua (C5) and CALIOP (V2 & V3) aerosol  
691 optical depth. Atmospheric Chemistry and Physics, 12(6), 3025–3043.  
692 <https://doi.org/https://doi.org/10.5194/acp-12-3025-2012>, 2012.

693 Reid, J.S., Eck, T. F., Christopher, S. A., Hobbs, P. V., and Holben B. R.: Use of the Angstrom  
694 exponent to estimate the variability of optical and physical properties of aging smoke  
695 particles in Brazil, *J. Geophys. Res.*, *104*, 27,489-27,489, 1999.

696 Remer, L. A., and coauthors: Global aerosol climatology from the MODIS satellite sensors, *J.*  
697 *Geophys. Res.*, *113*, D14S07, doi: 10.1029/2007JD009661, 2008.

698 Remer, L.A., Y.J. Kaufman, D. Tanré, S. Mattoo, D.A. Chu, J.V. Martins, R. Li, C. Ichoku,  
699 R.C. Levy, R.G. Kleidman, T.F. Eck, E. Vermote, and B.N. Holben, [The MODIS Aerosol](#)  
700 [Algorithm, Products, and Validation](#). *J. Atmos. Sci.*, **62**, 947–973,  
701 <https://doi.org/10.1175/JAS3385.1>, 2005.

702 Ryder, C. L., McQuaid, J. B., Flamant, C., Rosenberg, P. D., Washington, R., Brindley, H. E.,  
703 Highwood, E. J., Marsham, J. H., Parker, D. J., Todd, M. C., Banks, J. R., Brooke, J. K.,  
704 Engelstaedter, S., Estelles, V., Formenti, P., Garcia-Carreras, L., Kocha, C., Marengo, F.,  
705 Sodemann, H., Allen, C. J. T., Bourdon, A., Bart, M., Cavazos-Guerra, C., Chevaillier, S.,  
706 Crosier, J., Darbyshire, E., Dean, A. R., Dorsey, J. R., Kent, J., O'Sullivan, D., Schepanski,  
707 K., Szpek, K., Trembath, J., and Woolley, A.: Advances in understanding mineral dust and  
708 boundary layer processes over the Sahara from Fennec aircraft observations, *Atmos. Chem.*  
709 *Phys.*, *15*, 8479-8520, <https://doi.org/10.5194/acp-15-8479-2015>, 2015.

710 Shi Y., Zhang, J., Reid, J. S., Hyer, E., and Hsu, N. C.: Critical evaluation of the MODIS Deep  
711 Blue aerosol optical depth product for data assimilation over North Africa, *Atmos. Meas.*  
712 *Tech.*, *6*, 949-969, doi:10.5194/amt-6-949-2013, 2013.

713 Shi Y., Zhang J., Reid J. S., Hyer E. J., Eck T. F., and Holben B. N.: A critical examination of  
714 spatial biases between MODIS and MISR aerosol products – application for potential  
715 AERONET deployment, *Atmos. Meas. Tech.*, *4*, 2823–2836, 2011.

716 Stephens, G. L., and coauthors: The CLOUDSAT mission and the A-TRAIN, Bulletin of the  
717 American Meteorological Society, 83(12), 1771–1790. [https://doi.org/10.1175/BAMS-83-](https://doi.org/10.1175/BAMS-83-12-1771)  
718 [12-1771](https://doi.org/10.1175/BAMS-83-12-1771), 2002.

719 [Tackett, J. L., Winker, D. M., Getzewich, B. J., Vaughan, M. A., Young, S. A., and Kar, J.:](#)  
720 [CALIPSO lidar level 3 aerosol profile product: version 3 algorithm design, Atmos. Meas.](#)  
721 [Tech., 11, 4129-4152, https://doi.org/10.5194/amt-11-4129-2018, 2018.](#)

722 Tiwari, S., Srivastava, A. K., Bisht, D. S., Parmita, P., Srivastava, M. K., and Atri, S. D.:  
723 Diurnal and seasonal variation of black carbon and PM<sub>2.5</sub> over New Delhi, India:  
724 Influence of meteorology, Atmos. Res, 125, 50-62, doi:10.1016/j.atmos.res.2013.01.011,  
725 2013.

726 Toth, T. D., Campbell, J. R., Reid, J. S., Tackett, J. L., Vaughan, M. A., Zhang, J., & Marquis,  
727 J. W.: Minimum aerosol layer detection sensitivities and their subsequent impacts on  
728 aerosol optical thickness retrievals in CALIPSO level 2 data products. Atmospheric  
729 Measurement Techniques, 11(1), 499–514. [https://doi.org/https://doi.org/10.5194/amt-11-](https://doi.org/https://doi.org/10.5194/amt-11-499-2018)  
730 [499-2018](https://doi.org/https://doi.org/10.5194/amt-11-499-2018), 2018.

731 Toth, T. D., Zhang, J., Campbell, J. R., Reid, J. S., & Vaughan, M. A.: Temporal variability of  
732 aerosol optical thickness vertical distribution observed from CALIOP, Journal of  
733 Geophysical Research: Atmospheres, 121(15), 9117–9139.  
734 <https://doi.org/10.1002/2015JD024668>, 2016.

735 [Vaughan, M., Garnier, A., Josset, D., Avery, M., Lee, K.-P., Liu, Z., Hunt, W., Pelon, J., Hu,](#)  
736 [Y., Burton, S., Hair, J., Tackett, J. L., Getzewich, B., Kar, J., and Rodier, S.: CALIPSO](#)  
737 [lidar calibration at 1064 nm: version 4 algorithm, Atmos. Meas. Tech., 12, 51-82,](#)  
738 <https://doi.org/10.5194/amt-12-51-2019>, 2019.

739 Wang, J., Liu, X., Christopher, S. A., Reid, J. S., Reid, E. A., and Maring, H.: The effects of  
740 non-sphericity on geostationary satellite retrievals of dust aerosols, *Geophys. Res. Lett.*,  
741 30(24), 2293, doi:10.1029/2003GL018697, 2003.

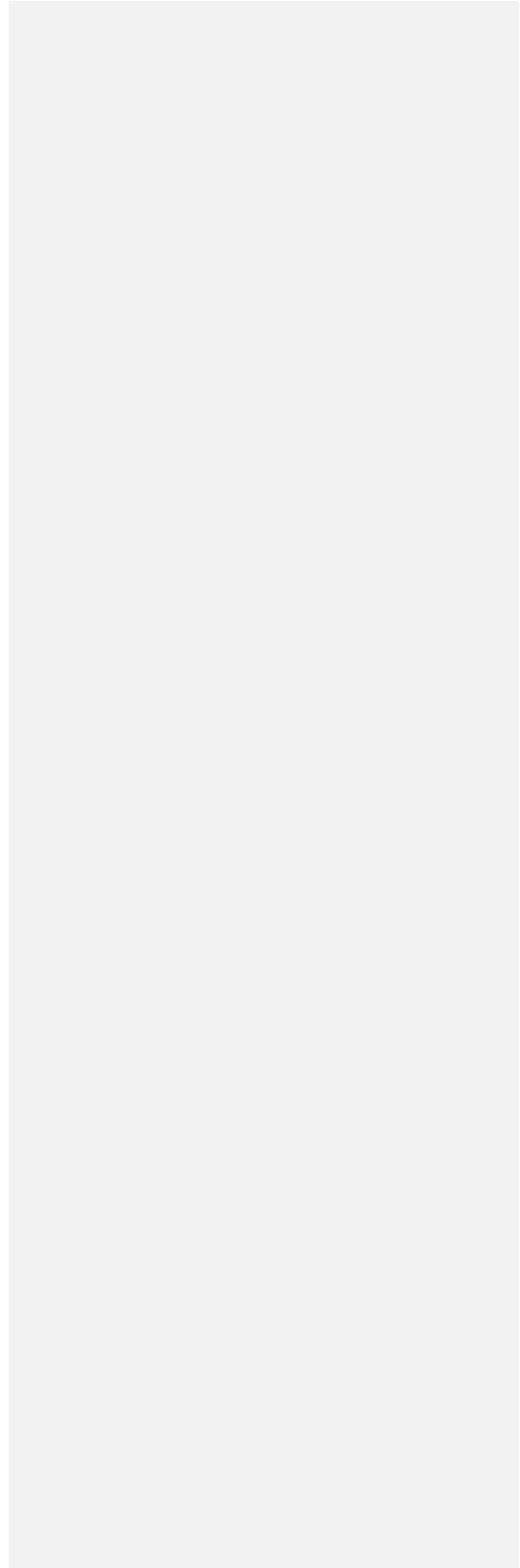
742 Winker, D. M., and coauthors: Overview of the CALIPSO Mission and CALIOP Data  
743 Processing Algorithms. *Journal of Atmospheric and Oceanic Technology*, 26(11), 2310–  
744 2323. <https://doi.org/10.1175/2009JTECHA1281.1>, 2009.

745 Young, S. A., M. A. Vaughan, R. E. Kuehn, and D. M. Winker, 2013: The Retrieval of Profiles  
746 of Particulate Extinction from Cloud-Aerosol Lidar Infrared Pathfinder Satellite  
747 Observations (CALIPSO) Data: Uncertainty and Error Sensitivity Analyses, *J. Atmos.*  
748 *Oceanic Technol.*, 30, 395-428, doi:10.1175/JTECH-D-12-00046.1.Yorks, J. E., P.A.  
749 Selmer, E.P. Nowottnick, S.D. Rodier, M.A. Vaughan, N. Dacic, M.J. McGill, and S.P.  
750 Palm, CATS Level 2 Vertical Feature Mask Algorithms and Data Products: An Overview  
751 and Initial Assessment, *Atmos. Meas. Tech. Discuss.*, in preparation, 2019.

752 Yorks, J. E., McGill, M. J., Palm, S. P., Hlavka, D. L., Selmer, P. A., Nowottnick, E., Vaughan,  
753 M. A., Rodier, S., and Hart W. D.: An Overview of the CATS Level 1 Data Products and  
754 Processing Algorithms, *Geophys. Res. Lett.*, 43, doi:[10.1002/2016GL068006](https://doi.org/10.1002/2016GL068006), 2016.

755 Yoshida M., Kikuchi, M., Nagao, T. M., Murakami, H., Nomaki, T., and Higurashi, A.:  
756 Common Retrieval of Aerosol Properties for Imaging Satellite Sensors, *Journal of the*  
757 *Meteorological Society of Japan*. Ser. II, Article ID 2018-039, [Advance publication],  
758 <https://doi.org/10.2151/jmsj.2018-039>, 2018.

759 Zhao, X. J., Zhang, X. L., Xu, X. F., Xu, J., Meng, W., and Pu, WW.: Seasonal and diurnal  
760 variation of ambient PM<sub>2.5</sub> concentrations in urban and rural environments in Beijing,  
761 *Atmos. Environ.*, 43, 2893-2900, doi: 10.106/j.atmosenv.2009.03.009., 2009.



763 Table 1. Descriptive statistical properties between collocated CATS and AERONET, CALIOP  
 764 and Aqua MODIS AOD retrievals. Here STDDEV indicates standard deviation of AOD and R-  
 765 value represents the correlation coefficient.

Sensor	No. of Points	Slope	R-value	Mean AOD	Median AOD	Max AOD	Min AOD	STDDEV	CATS Mean AOD	CATS Median AOD	CATS Max AOD	CATS Min AOD	CATS STDDEV
AERONET	2240	0.56	0.65	0.088	0.054	0.98	0.001	0.103	0.099	0.058	1.31	0.0004	0.119
MODIS Aqua	3529	0.7	0.74	0.067	0.048	0.81	0.0004	0.07	0.07	0.053	1.76	0.002	0.075
MODIS Terra	2334	0.74	0.72	0.076	0.056	0.9	0.0013	0.081	0.084	0.065	1.13	0.0063	0.079
CALIOP	2762	0.74	0.74	0.089	0.063	1.01	0	0.102	0.092	0.065	1.1	0.0018	0.1

766  
767

768 Table 2. Sensitivity study of descriptive statistical properties between collocated CATS and  
 769 AERONET, CALIOP and Aqua MODIS AOD retrievals by varying spatial and temporal  
 770 collocation windows. Here STDDEV indicates standard deviation of AOD and R-value  
 771 represents the correlation coefficient.

Collocation Thresholds Spatial (30 min.)	AERONET/CATS				AERONET				CALIOP				CATS					
	No. of Points	Slope	R-value	Mean AOD	Median AOD	Max AOD	Min AOD	STDDEV	Mean AOD	Median AOD	Max AOD	Min AOD	STDDEV	Mean AOD	Median AOD	Max AOD	Min AOD	STDDEV
0.2°	904	0.54	0.63	0.092	0.052	0.82	0.002	0.107	0.102	0.058	1.31	0.004	0.124	0.069	0.052	1.76	0.003	0.078
0.4°	2240	0.56	0.65	0.088	0.054	0.98	0.001	0.103	0.099	0.058	1.31	0.004	0.119	0.07	0.053	1.76	0.002	0.075
0.8°	5114	0.53	0.63	0.087	0.052	0.98	0.001	0.105	0.096	0.056	2	0.004	0.125	0.069	0.054	1.76	0.003	0.074
<b>Temporal (0.4° lat./lon.)</b>																		
15 minutes	1931	0.54	0.63	0.089	0.053	0.98	0.001	0.105	0.1	0.057	1.33	0.004	0.123	0.069	0.052	1.76	0.003	0.078
30 minutes	2240	0.56	0.65	0.088	0.054	0.98	0.001	0.103	0.099	0.058	1.31	0.004	0.119	0.07	0.053	1.76	0.002	0.075
60 minutes	2695	0.55	0.64	0.087	0.053	0.98	0.001	0.103	0.096	0.057	1.37	0.006	0.118	0.069	0.054	1.76	0.003	0.074
<b>Collocation Thresholds Spatial (30 min.)</b>																		
<b>Temporal (0.4° lat./lon.)</b>																		
15 minutes	1392	0.76	0.77	0.09	0.063	0.95	0	0.104	0.092	0.066	1.1	0.0024	0.102	0.069	0.052	1.74	0.003	0.075
30 minutes	2762	0.74	0.74	0.089	0.063	1.01	0	0.102	0.092	0.065	1.1	0.0018	0.1	0.07	0.053	1.76	0.002	0.075
60 minutes	5602	0.74	0.75	0.09	0.063	1.4	0	0.104	0.093	0.066	1.53	0.0007	0.103	0.069	0.054	1.71	0.003	0.073
<b>Collocation Thresholds Spatial (30 min.)</b>																		
<b>Temporal (0.4° lat./lon.)</b>																		
15 minutes	1814	0.61	0.71	0.064	0.048	0.82	0.0004	0.067	0.069	0.052	1.33	0.0004	0.119	0.069	0.052	1.76	0.003	0.078
30 minutes	3529	0.70	0.74	0.067	0.048	0.81	0.0004	0.07	0.07	0.053	1.31	0.0004	0.119	0.069	0.052	1.76	0.002	0.075
60 minutes	6490	0.78	0.76	0.069	0.049	1.21	0.0004	0.077	0.072	0.054	1.76	0.003	0.074	0.069	0.054	1.76	0.003	0.074

775 Table 3. CALIOP and CATS mean AODs / AOD standard deviations for regions as highlighted  
 776 in Figure 6 and globally between +/- 52° latitude.

Region	Latitude	Longitude	Mean CATS AOD (DJFMAM/JJASON)	Mean CALIOP AOD (DJFMAM/JJASON)	Mean CATS Standard Deviation (DJFMAM/JJASON)	Mean CALIOP Standard Deviation (DJFMAM/JJASON)
Global	52°S-52°N	180°W-180°E	0.09/0.10	0.09/0.09	0.037/0.039	0.036/0.034
India	7.5°N - 32.5°N	65°E - 85°E	0.22/0.26	0.22 /0.28	0.068/0.072	0.072/0.078
Africa - North	2.5°N - 22.5°N	35°W - 20°E	0.25/0.24	0.30 /0.25	0.062/0.064	0.075/0.067
Africa - South	17.5°S - 2.5°N	0° - 30°E	0.12/0.20	0.15 /0.13	0.037/0.048	0.038/0.038
Middle East	12.5°N - 27.5°N	35°E - 50°E	0.23/0.35	0.26/0.35	0.076/0.099	0.082/0.091
China	27.5°N - 37.5°N	110°E - 120°E	0.20/0.17	0.21 /0.16	0.061/0.056	0.074/0.060

777

778

779

780

781

782

783 Table 4. Geographic ranges, height above ground level of maximum extinction, diurnal  
 784 extinction range at height of maximum extinction, and time (local) of peak extinction for the  
 785 boxed red regions in Figure 6 and vertical profiles shown in Figures 12 and 13.

DJFMAM/JJASON					
Region	Latitude	Longitude	Height AGL (m) of Max. Extinction	Extinction Range ( $\text{km}^{-1}$ ) at Height AGL of Max. Extinction	Time of Peak Extinction at Height AGL of Max. Extinction
India	7.5°N - 32.5°N	65°E - 85°E	180/360	0.099-0.136/0.135-0.163	0 am/6 am
Africa - North	2.5°N - 22.5°N	35°W - 20°E	420/420	0.107-0.121/0.082-0.113	6 am/6 am
Africa - South	17.5°S - 2.5°N	0° - 30°E	/420	/0.092-0.126	/6 am
Middle East	12.5°N - 27.5°N	35°E - 50°E	180/240	0.075-0.121/0.086-0.156	0 am/0 am
China	27.5°N - 37.5°N	110°E - 120°E	180/240	0.098-0.148/0.086-0.132	6 am/6 am

786

787

788

789

790 **Figure Captions**

791  
792 **Figure 1.** Collocated AERONET 1020 nm AOT vs. CATS 1064 nm AOD a) without CATS QA  
793 applied, and b) with CATS QA applied.

794 **Figure 2.** Collocated MODIS C6.1 a) Terra and b) Aqua estimated 1064 nm AOD vs. CATS  
795 1064 nm AOD with CATS QA applied.

796 **Figure 3.** Collocated CALIOP 1064 nm AOD vs. CATS 1064 nm AOD with CATS QA applied  
797 for a) both day and night, b) nighttime over-land, c) nighttime over-water, d) daytime over-land,  
798 e) daytime over-water.

799 **Figure 4:** CATS 1064 nm AOD a) as a function of local time for the globe, and b) as a function  
800 of local time for areas south of -25 degrees. The difference between CATS 1064 nm AOD and  
801 AERONET 1020 nm AOD as a function of local time is shown in c). The mean is represented  
802 by the blue line, while the median is the green line.

803 **Figure 5.** CATS and CALIOP vertical profiles of 1064 nm extinction for a) all profiles, b)  
804 daytime only, c) nighttime only, d) over-water, and e) over land. f) Difference between CATS  
805 and CALIOP mean 1064 nm extinction for all collocated profiles (5a) as a function of height.  
806 Mean AOD values are as follows: for CATS: a) 0.094 , b) 0.091 , c) 0.098, d) 0.088, e) 0.119,  
807 and for CALIOP: a) 0.093, b) 0.092, c) 0.093, d) 0.084, e) 0.127.

808 **Figure 6.** Mean AOD (1064 nm) by season for a) DJFMAM CATS, b) JJASON CATS, c)  
809 DJFMAM CALIOP, d) JJASON CALIOP, e) DJFMAM MODIS Aqua, and f) JJASON MODIS  
810 Aqua. Red boxes indicate locations of regional vertical distributions in Figures 12 and 13.

811 **Figure 7.** Mean CATS AOD (1064 nm) by season for a) DJFMAM below 1 km AGL, b)  
812 JJASON below 1 km AGL, c) DJFMAM 1-2 km AGL, d) JJASON 1-2 km AGL, e) DJFMAM  
813 above 2 km AGL, and f) JJASON above 2 km AGL.

814 **Figure 8.** Seasonal Mean AOD (1064 nm) binned by every 6-hours for a) DJFMAM 0 UTC, b)  
815 JJASON 0 UTC, c) DJFMAM 6 UTC, d) JJASON 6 UTC, e) DJFMAM 12 UTC, f) JJASON 12  
816 UTC, g) DJFMAM 18 UTC, and h) JJASON 18 UTC.

817 **Figure 9.** Maximum minus minimum mean seasonal AOD (1064 nm) for a) DJFMAM, and b)  
818 JJASON.

819 **Figure 10.** Global mean 6-hourly vertical profiles of CATS 1064 nm extinction for a) DJFMAM  
820 all profiles, b) DJFMAM water profiles, c) DJFMAM not-water profiles, e) JJASON all profiles,  
821 f) JJASON water profiles, g) JJASON not-water profiles. Mean AODs are as follows: a) 0.084,  
822 b) 0.078, c) 0.098, d) 0.089, e) 0.082, and f) 0.102.

823 **Figure 11.** Global mean 6-hourly local time (0:00 am, 6:00 am, 12:00 pm and 6:00 pm) vertical  
824 profiles of CATS 1064 nm extinction for a) DJFMAM all profiles, b) DJFMAM water profiles, c)  
825 DJFMAM not-water profiles, d) JJASON all profiles, e) JJASON water profiles, f) JJASON not-  
826 water profiles. Mean AODs are as follows: a) 0.080, b) 0.079, c) 0.095, d) 0.082, e) 0.081, and f)  
827 0.105.

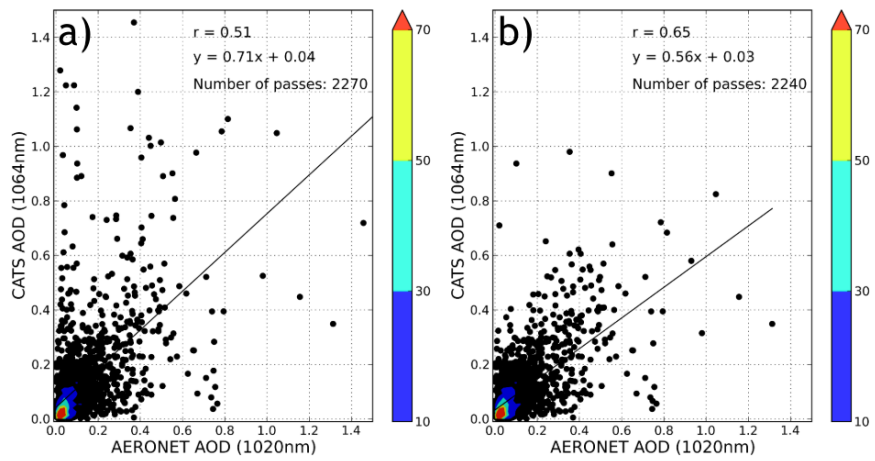
828

829 **Figure 12.** DJFMAM 6-hourly average (local time; 0:00 am, 6:00 am, 12:00 pm and 6:00 pm)  
830 vertical profiles of CATS 1064 nm for locations shown in Figure 6a; a) Africa-north, b) Middle  
831 East, c) India, and d) Northeast China.

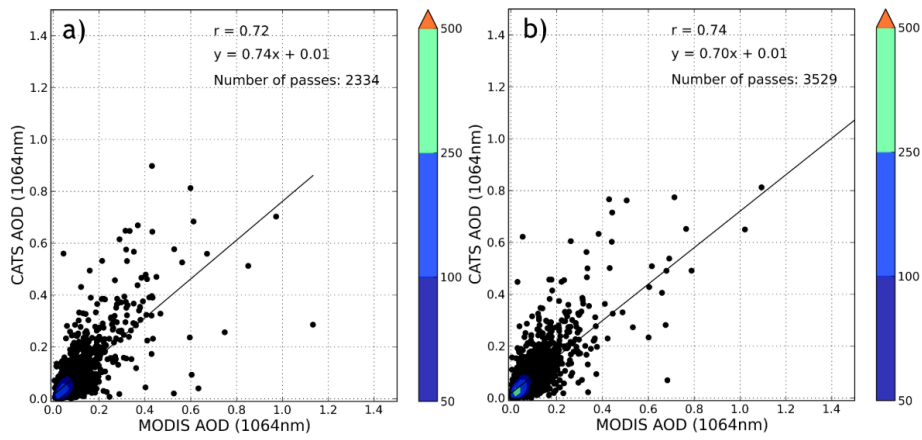
832

833 **Figure 13.** JJASON 6-hourly average (local time; 0:00 am, 6:00 am, 12:00 pm and 6:00 pm)  
834 vertical profiles of CATS 1064 nm for locations shown in Figure 6b; a) Africa-north, b) Africa-  
835 south, c) Middle East, d) India, and e) Northeast China.

836

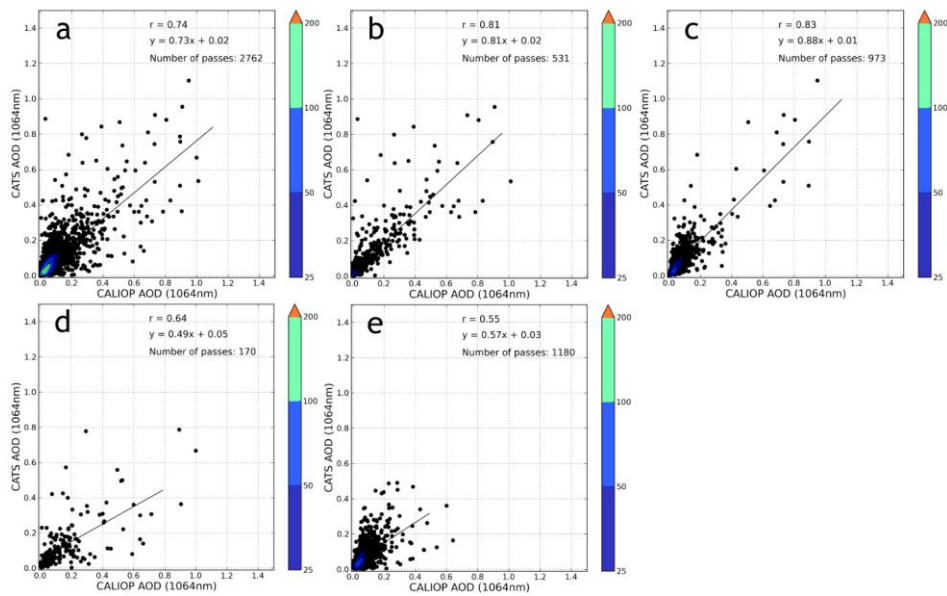


837  
 Figure 1. Collocated AERONET 1020 nm AOT vs. CATS 1064 nm AOD a) without CATS QA applied, and b) with CATS QA applied.



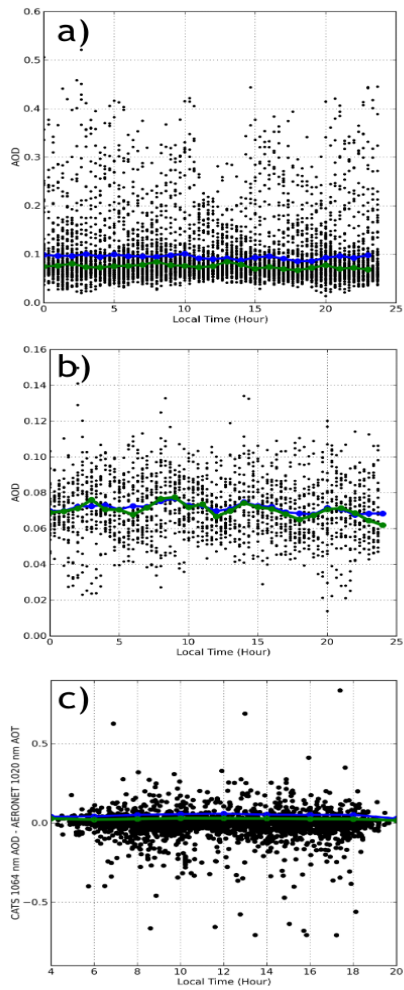
838

Figure 2. Collocated MODIS C6.1 a) Terra and b) Aqua estimated 1064 nm AOD vs. CATS 1064 nm AOD with CATS QA applied.



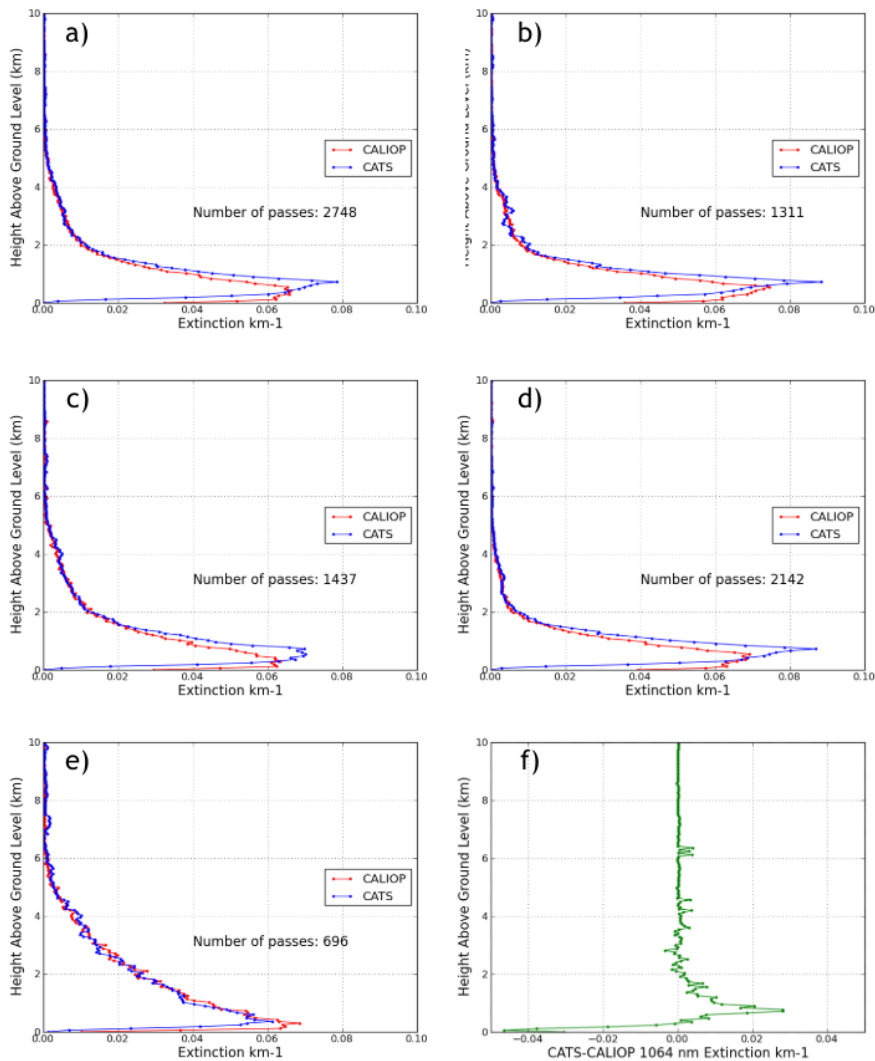
839

Figure 3. Collocated CALIOP 1064 nm AOD vs. CATS 1064 nm AOD with CATS QA applied for a) both day and night, b) nighttime over-land, c) nighttime over-water, d) daytime over-land, e) daytime over-water.



840

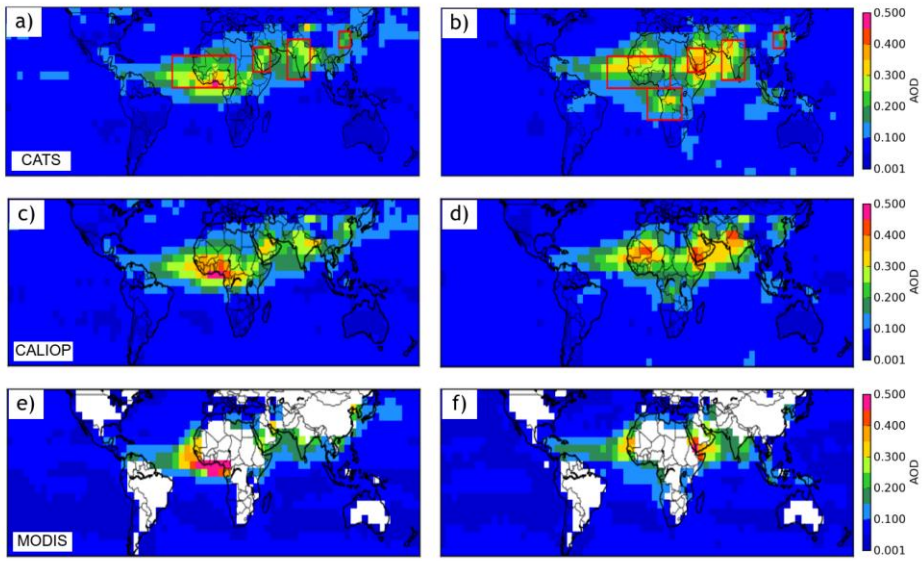
Figure 4. CATS 1064 nm AOD a) as a function of local time for the globe, and b) as a function of local time for areas south of -25 degrees. The difference between CATS 1064 nm AOD and AERONET 1020 nm AOD as a function of local time is shown in c). The mean is represented by the blue line, while the median is the green line.



841

Figure 5. CATS and CALIOP vertical profiles of 1064 nm extinction for a) all profiles, b) daytime only, c) nighttime only, d) over-water, and e) over land. **f) Difference between CATS and CALIOP mean 1064 nm extinction for all collocated profiles (5a) as a function of height.** Mean AOD values are as follows: for CATS: a) 0.094, b) 0.091, c) 0.098, d) 0.088, e) 0.119, and for CALIOP: a) 0.093, b) 0.092, c) 0.093, d) 0.084, e) 0.127.

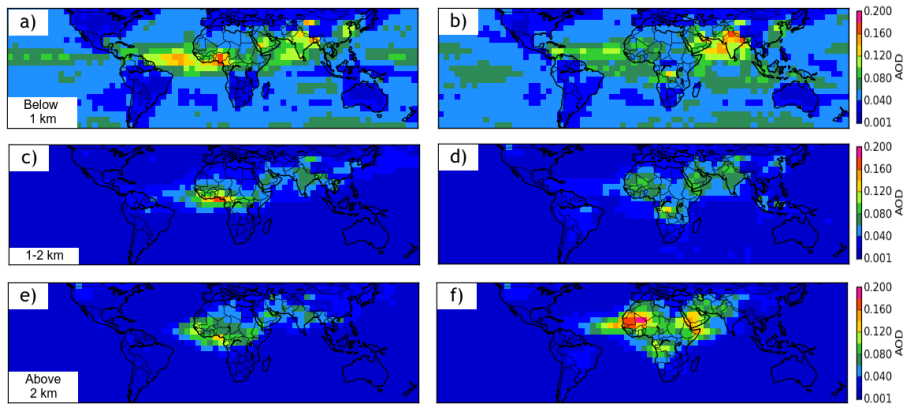
Formatted: Font color: Auto



842  
843

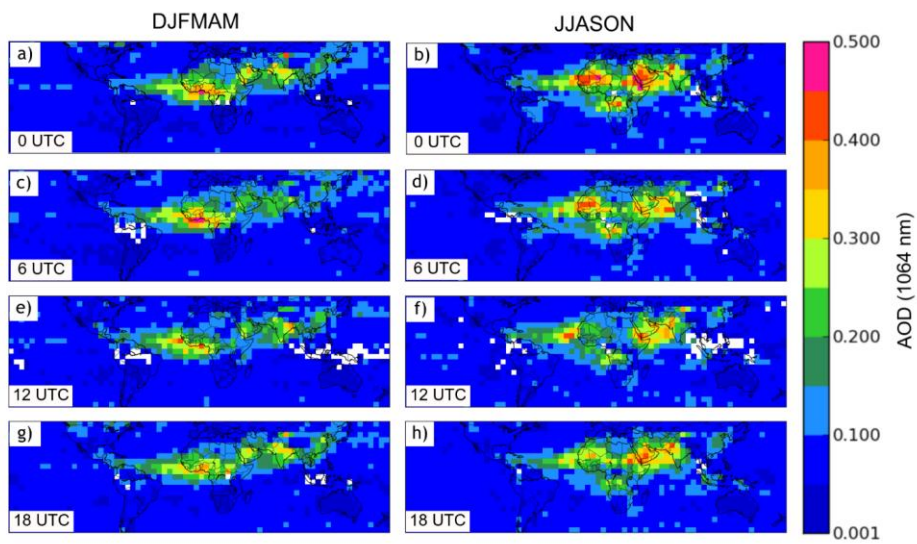
Figure 6. Mean AOD (1064 nm) by season for a) DJFMAM CATS, b) JJASON CATS, c) DJFMAM CALIOP, d) JJASON CALIOP, e) DJFMAM MODIS Aqua, and f) JJASON MODIS Aqua. Red boxes indicate locations of regional vertical distributions in Figures 12 and 13.

844  
845  
846  
847  
848



849

Figure 7. Mean CATS AOD (1064 nm) by season for a) DJFMAM below 1km AGL, b) JJASON below 1 km AGL, c) DJFMAM 1-2 km AGL, d) JJASON 1-2 km AGL, e) DJFMAM above 2 km AGL, and f) JJASON above 2 km AGL.



850

Figure 8. Seasonal Mean AOD (1064 nm) binned by every 6-hours for a) DJFMAM 0 UTC, b) JJASON 0 UTC, c) DJFMAM 6 UTC, d) JJASON 6 UTC, e) DJFMAM 12 UTC, f) JJASON 12 UTC, g) DJFMAM 18 UTC, and h) JJASON 18 UTC.

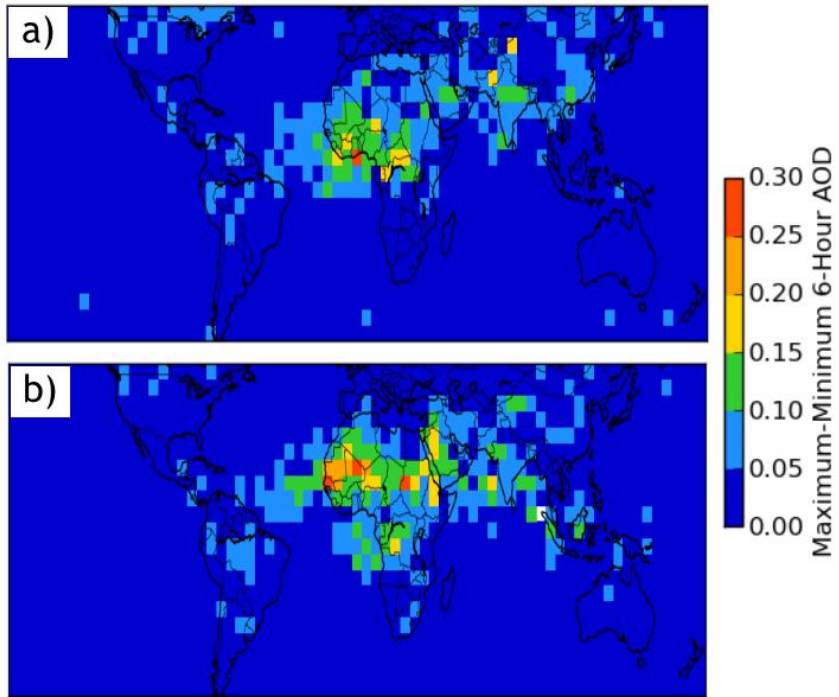
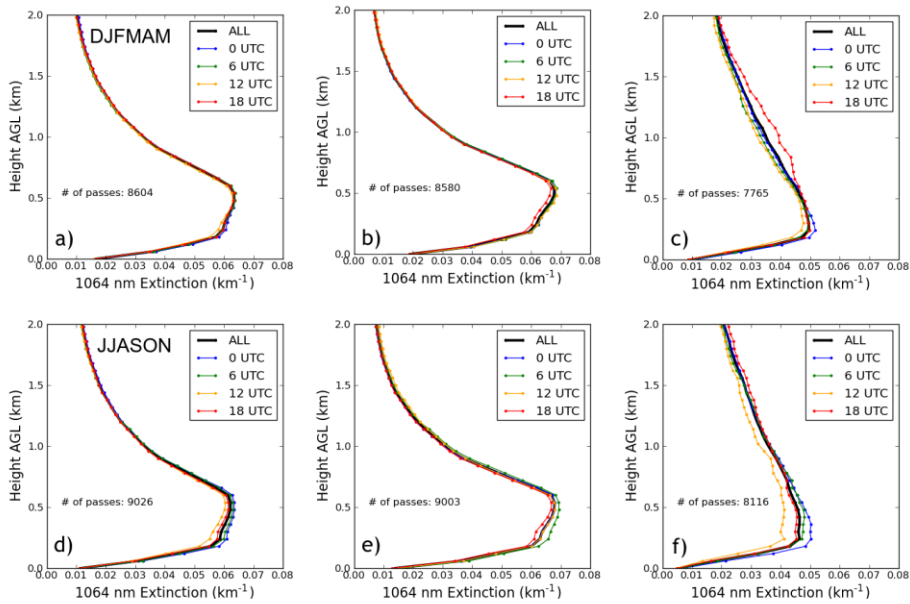


Figure 9. Maximum minus minimum mean seasonal AOD (1064 nm) for a) DJFMAM, and b) JJASON.

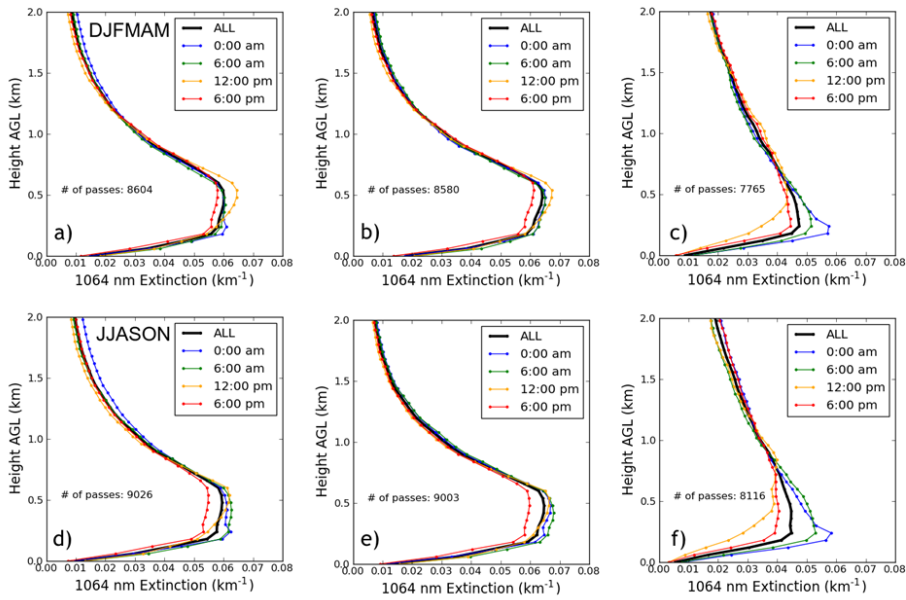


853

854

Figure 10. Global mean 6-hourly vertical profiles of CATS 1064 nm extinction for a) DJFMAM all profiles, b) DJFMAM water profiles, c) DJFMAM not-water profiles, d) JJASON all profiles, e) JJASON water profiles, f) JJASON not-water profiles. Mean AODs are as follows: a) 0.084, b) 0.078, c) 0.098, d) 0.089, e) 0.082, and f) 0.102.

855



856

857

858

859

860

861

862

863

864

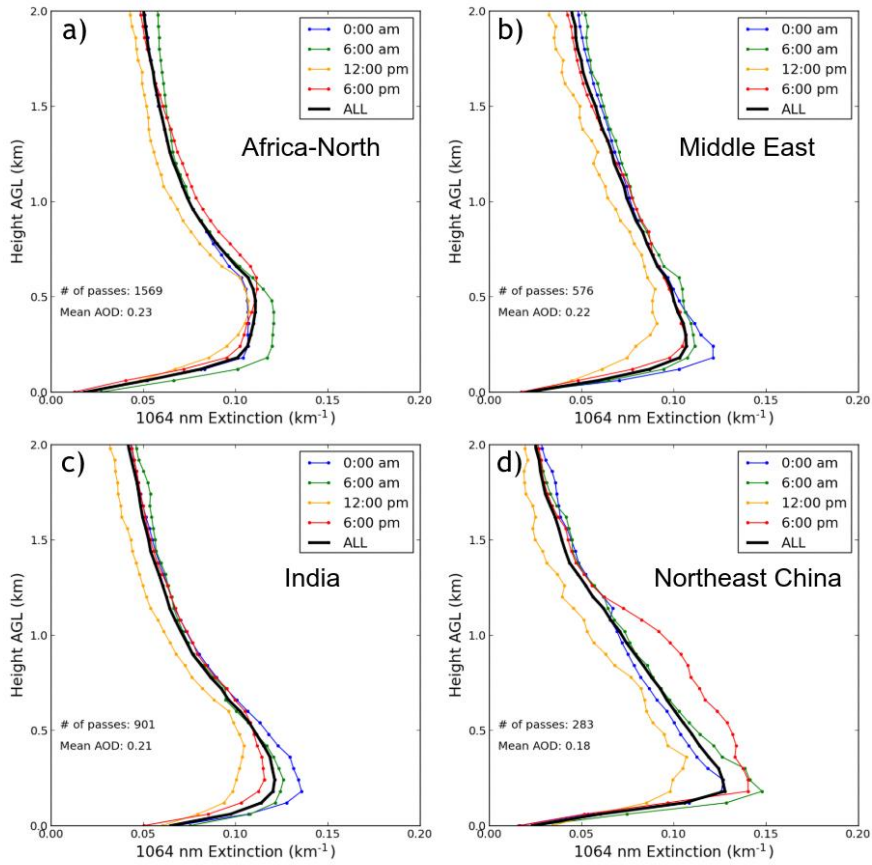
865

866

867

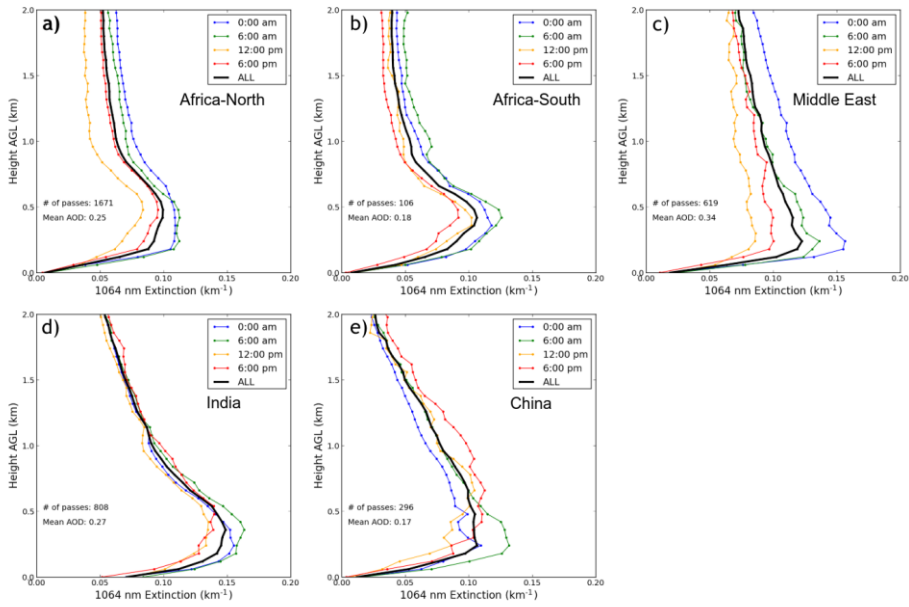
868

Figure 11. Global mean 6-hourly local time (0:00 am, 6:00 am, 12:00 pm and 6:00 pm) vertical profiles of CATS 1064 nm extinction for a) DJFMAM all profiles, b) DJFMAM water profiles, c) DJFMAM not-water profiles, d) JJASON all profiles, e) JJASON water profiles, f) JJASON not-water profiles. [Mean AODs are as follows: a\) 0.080, b\) 0.079, c\) 0.095, d\) 0.082, e\) 0.081, and f\) 0.105.](#)



869  
 870 Figure 12. DJFMAM 6-hourly average (local time; 0:00 am, 6:00 am, 12:00 pm and 6:00  
 871 pm) vertical profiles of CATS 1064 nm for locations shown in Figure 6a; a) Africa-north,  
 b) Middle East, c) India, and d) Northeast China.

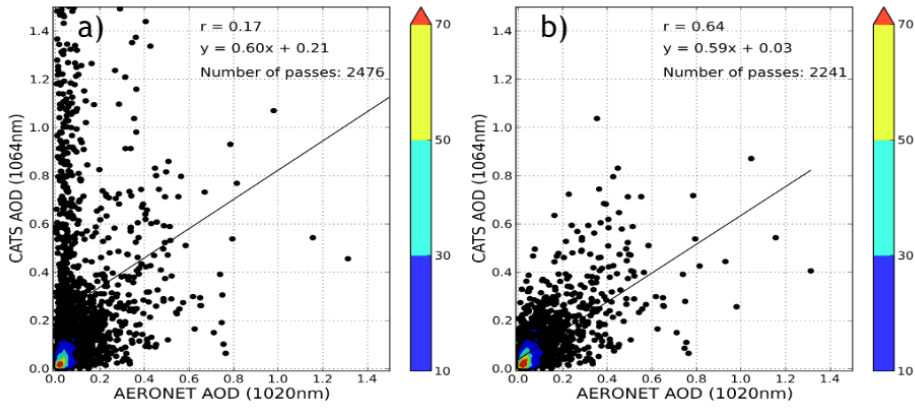
872  
 873  
 874  
 875  
 876  
 877



878

Figure 13. JJASON 6-hourly average (local time; 0:00 am, 6:00 am, 12:00 pm and 6:00 pm) vertical profiles of CATS 1064 nm for locations shown in Figure 6b; a) Africa-north, b) Africa-south, c) Middle East, d) India, and e) Northeast China.

879 Appendix A:  
880



881  
882  
883 Figure A1. Collocated AERONET 1020 nm AOT vs. CATS 1064 nm AOD a) without CATS  
884 QA applied, and b) with CATS QA applied. CATS V2-01 aerosol products were used in  
885 constructing this plot.

886